Polyoxomolybdates with Emergent Properties

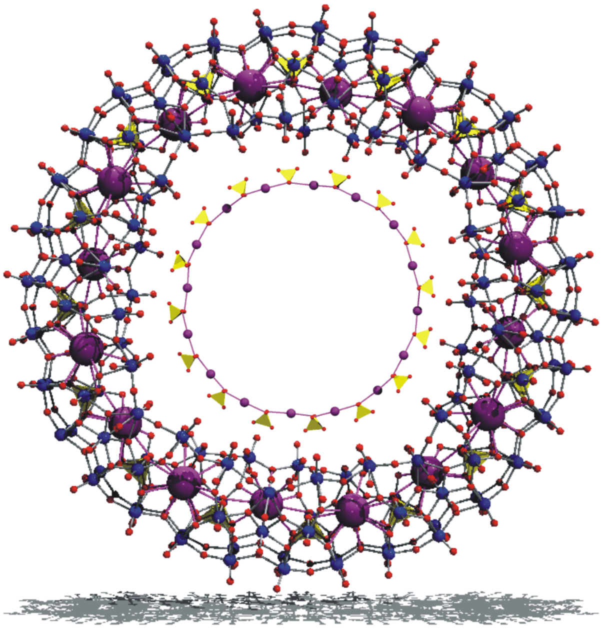

\- Cumulative Dissertation -

Liviu Dan Toma

Faculty of Chemistry
University of Bielefeld

May 2006

This thesis is the result of research carried out during the period of January 2002 to November 2005 under the supervision of Prof. Dr. Dr. h. c. mult. Achim Müller, Lehrstuhl für Anorganische Chemie I, Universität Bielefeld.

Referee: Prof. Dr. Dr. h.c. mult. Achim Müller

Second referee: Prof. Dr. Lothar Weber

To my beloved wife Agnieszka and my family.

Acknowledgement

I wish to thank my supervisor Prof. Dr. Dr. h.c. mult. Achim Müller for the provision of a challenging and rewarding project, for his guidance as well as the provision of financial support during the course of this investigation.

I am especially grateful to Dr. Hartmut Bögge and Marc Schmidtmann for their help with the X-ray diffraction measurements and crystal structure determinations, this thesis would not have been possible without their cooperation and help.

A number of people have made the challenge of completing doctoral studies in a foreign land possible and enjoyable. My special thanks in this regard go especially to Dr. Alice Merca and Dr. Soumyajit Roy, for their friendship, support, and for many interesting discussions about chemistry and beyond. I am also extremely grateful to Ms. K. Lacey and Dr. E. Diemann for being there always in my hours of need.

I gratefully acknowledge Ms. G. Heinze-Brückner for her diligence, help and cooperation in the measurement of countless infrared and Raman spectra. Thanks are also due to Ursula Stuphorn for measurement of the UV-Vis spectra and Brigitte Michel for the C, H, N analysis and Alois Berckle for natrium analysis.

I am thankful further to numerous other friends and colleagues who made this stay in Bielefeld a beautiful one, my thanks in this regard go to Dr. E. Beckmann, Dr. A. Bell, Dr. B. Botar, Ms. M. Brusch, Dr. M. Fricke, Dr. M. Harms, Ms. M. Czerwinska, Mr. T. Mitra, Mr. B. Ostheider, Dr. K. Schneider, Mr. C. Schäffer, Ms. F. Sousa, Ms. A.M Todea and Dr. R. Tomsa.

This thesis would not have been possible without the generous financial support of 'Graduiertenkolleg Strukturbildungsprozesse', University of Bielefeld. I would also like to express my gratitude to Prof. A. Dress and Prof. W.- J. Beyn, the directors of the 'GK' for their continuous support.

Final word of gratitude goes to my wife Agnieszka and to my family.

The Figure on the cover depicts the synergetic activation of "silent receptor" sites leading to a new type of inclusion complex: integration of a 64-membered ring comprising K^+ and SO_4^{2-} ions into the ring-type molybdenum oxide-based nanoobject (ball and stick representation) highlighting the K centers (pink spheres) and SO_4^{2-} units (yellow; polyhedral representation). For a better demonstration of the $K^+ - SO_4^{2-}$ type interaction, the structure of the $\{K(SO_4)\}_{16}$ ring on a smaller scale and removed from its environment is shown in the center (O red, Mo blue). For details refer to Chapter 2.

Contents

1 Introduction **1**

1.1 Synopsis 1
1.2 State of the art 2
  1.2.1 Polyoxomolybdate clusters: giant wheels and balls 3
1.3 Goals of the project: defining the problem 6

2 Publications **10**

2.1 *Synergetic activation of "silent receptor" sites leading to a new type of inclusion complex: integration of a 64-membered ring comprising K^+ and SO_4^{2-} ions into a molybdenum oxide-based nanoobject*
A. Müller, *L. Toma*, H. Bögge, M. Schmidtmann and P. Kögerler
Chem. Commun., **2003**, 2000. 11
2.2 *Porous Capsules Allow Pore Opening and Closing That Results in Cation Uptake*
A. Müller, *L. Toma*, H. Bögge, C. Schäffer and A. Stammler
Angew. Chem. Int. Ed., **2005**, 44, 7757. 12
2.3 *Reactions inside a porous nanocapsule/artificial cell: encapsulates' structuring directed by internal surface deprotonations*
A. Müller, *L. Toma*, H. Bögge, M. Henry, E. T. K. Haupt, A. Mix and F. L. Sousa
Chem. Commun., **2006**, 3396. 13

3 Summary and conclusion **14**

4 Curriculum Vitae **16**

Chapter 1

Introduction

1.1 Synopsis

The control of the aggregation processes in supramolecular inorganic chemistry is one of the keys for the targeted synthesis of mesoscopic materials with a high level of complexity. Since these materials are often in the nanometer size-regime, supramolecular chemistry is generally thought also as a (sub-)discipline of "Nanoscience", which is a popular research discipline even though a clear-cut definition is not straightforward. This is mainly because of the interdisciplinary nature of this field. Nanoscience involves physics, chemistry, and biochemistry. In view of this, it is natural that scientists which are trained in different fields will adopt different definitions. The word "nano" means 10^{-9} so a nanometer is one billionth of a meter. One general definition of nanoscience is that it concerns itself with the study of objects which are anywhere from tens to hundreds of nanometers in size. Figure 1.1 exemplifies very well the concept of nanoscience, which concerns itself with the study of materials with very small dimensions, materials found in nature as well as those man made.

The subject of this thesis is dealing with the structural chemistry of large polyoxometalates clusters, or simply POMs. Generally speaking, the chemist, and in particular the inorganic chemist concentrating on polyoxometalates, is in a position to connect elementary building blocks and their derivatives in different ways which enables him to synthesize a large variety of remarkable substances. Of particular importance in this context are the anionic-type species which have $\{MO_x\}$-type building-block units, where M stands for the d block elements in high oxidation states. POMs of large or extreme size have fascinating and extensive structural variety. Their structures are based upon different types of linking of $\{MO_x\}$ polyhedra, whereby the species are formed by a kind of self-assembly process. A fascinating aspect of the self-assembly process is that it can lead to aggregates, which can again be linked in different ways. This type of unit-construction principle seems to be archetypal for polyoxometalate chemistry. It is now possible to enter the "nanoworld" step-by-step by means of (directed) self-assembly processes. This designates the goal of current chemical research in this area, that of generating nanosized molecular materials from units with well-defined properties.

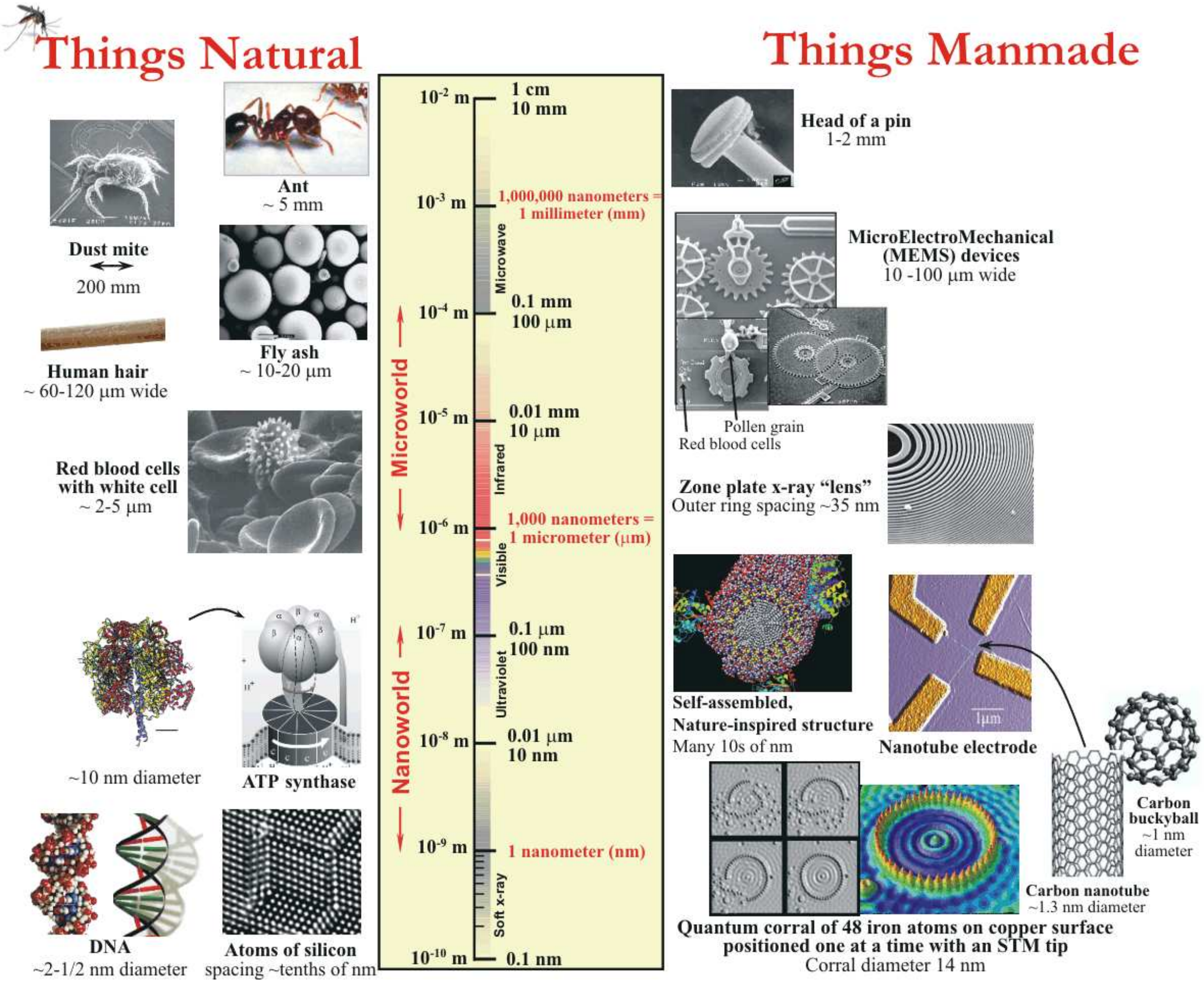

Figure 1.1: *The scale of things - Nanometers and more. Adapted from reference [1].*

1.2 State of the art

Polyoxometalates are well-defined, discrete transition metal oxide clusters with a large range of possible applications in fundamental and applied science including catalysis [2], electrochemistry [3], electrooptics [4], medicine [5], corrosion protection, dyes and pigments, dopants in (non-)conductive polymers and sol-gels, bleaching of paper pulp, as well as analytical chemistry [6]. In contrast to many semiconductor nanoparticles and quantum dots, POMs are strictly uniform at the atomic level. A bewildering variety of POM structures has been characterized since 1933, when the seminal X-ray crystal structure analysis of the Keggin anion, $[PW_{12}O_{40}]^{3-}$, appeared in the literature [7]. This work has recently culminated in the discovery of giant nanosized polyoxomolybdate [1] clusters $\{Mo_{132}\}$, $\{Mo_{154}\}$, $\{Mo_{176}\}$, $\{Mo_{368}\}$ [9, 10, 11, 12]. The exploitation of value-adding properties of POMs in advanced materials has remained elusive until recently, mainly due to the fact that these compounds are commonly obtained as crystalline solids. Recent studies show, however, that giant, spherical POM systems, including some wheel-shaped and hollow "Keplerate" species, spontaneously form "necklaces" and 2D layers by a solid state reaction and slowly self-assemble into a vesicle structure in polar solvents [13, 14, 15, 16, 17].

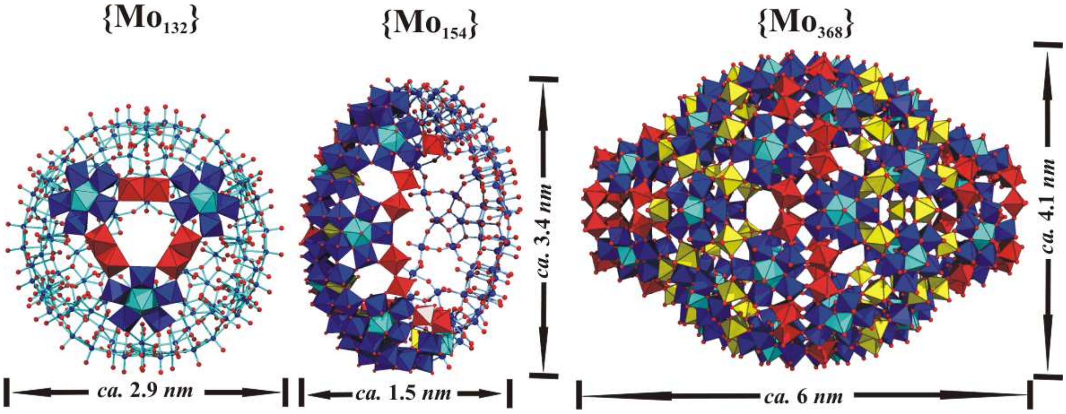

Figure 1.2: *A schematic representation showing the general architecture principle for the the giant nanosized polyoxomolybdate clusters - three important types of clusters are depicted in polyhedral and ball and stick representations:* $\{Mo_{132}\}$ *(left),* $\{Mo_{176}\}$ *(middle) and* $\{Mo_{368}\}$ *(right). The central pentagonal bipyramidal* $[(Mo)Mo_5]$ *unit is shown in cyan surrounded by five edge-shared octahedral units in blue; the edge and corner shared* $[Mo_2]$ *units with different composition are shown in red; and* $[Mo_1]$ *units in yellow polyhedral representation.*

1.2.1 Polyoxomolybdate clusters: giant wheels and balls

The challenge for the chemist is to synthesize complex multi-functional molecules under non-dissipative conditions using one-pot reactions, without the need to separate and purify each single intermediate product. The basis is constituted by a system with a variety of combinatorially linkable polyoxometalate (oxomolybdates) building units either as existing or virtual species (at disposition) which are available on demand in a kind of library depending on the boundary conditions. In the solution of oxomolybdates, controlled linking of metal-oxide building blocks produces a large variety of structures - and provide the option to form exquisite molecular architectures [18] with unprecedented functionalities. This only became evident in recent years [19]. Specifically speaking the reasons for such a versatile behavior of polyoxomolybdates are the following:

---

[1] Polyoxomolybdates are those polyoxometalates where the metal centers are molybdenum. The polyoxometalates can in turn be defined as a class of cluster anions comprising of at least two or more single or mixed-valent metal centers, each covalently bonded with oxygen atoms as per the requirement of coordinative saturation of the central metal atoms [8].

1. The easy change of coordination numbers as well as easy exchange of H_2O ligands at Mo sites.
2. The moderate strength of Mo-O-Mo type bonds allowing ”split and link” type processes.
3. The easy change and especially increase of electron densities without the strong tendency to form metal-metal bonds.
4. The presence of terminal Mo = O groups preventing in principle unlimited growth to extended structures ([11], see also: [20]).

In spite of an exotic architectural aspect (see Figure 1.2), synthetically speaking, [21] all the giant polyoxomolybdate based systems are very easy to handle.

A superfullerene (giant ball)

While molecular systems, even relatively large ones, can in principle be generated by successive steps of synthesis and isolation [22], the formation of extremely large molecular systems, in particular those with complex structures, interesting properties, together with very high symmetry, *e.g.* those comparable to simple spherical viruses, requires a different method of approach. If the intention is to construct for instance a giant species similar in size and shape to spherical viruses with icosahedral $(C_5\ \ C_3\ \ C_2)$ symmetry, we have to find a reaction system in which pentagonal units can first be generated, then get linked and get placed at the 12 corners of an icosahedron. In the case of polyoxomolybdates these pentagonal units ($\{(Mo)Mo_5\}$ groups) consist of a central bipyramidal $\{MoO_7\}$ unit sharing edges with five $\{MoO_6\}$ octahedra. When linkers in the form of dinuclear bridging units are present in solution, for instance those of the classical $\{Mo_2^VO_4\}^{2+}$ type [23] (typically formed in reduced molybdate solutions in the presence of bidentate ligands) that can link these pentagonal units, an icosahedral molecular system with 12 of the mentioned pentagons and 30 of the mentioned linkers is formed (details are presented in Figures 1.2 and 1.3). Moreover, most of these clusters (the spherical ones) can be manipulated keeping the robust nanoscopic oxomolybdate skeleton intact.

The ring molecular big-wheels: structural aspects

The $\{Mo_8\}$ building block, found in many large polyoxomolybdate structures, is itself (as mentioned above) built up by a densely packed pentagonal $\{(Mo)Mo_5\}$ type unit, containing a central MoO_7 sharing edges with five MoO_6 octahedra, and two more weakly bonded (sharing only corners) MoO_6 octahedra which can be more easily ’removed’. The pentagonal unit with its high formation tendency is, for instance, responsible for the formation of structures with icosahedral symmetry, like the $\{Mo_{132}\}$-type clusters (for details, see Figures 1.2 and 1.3).

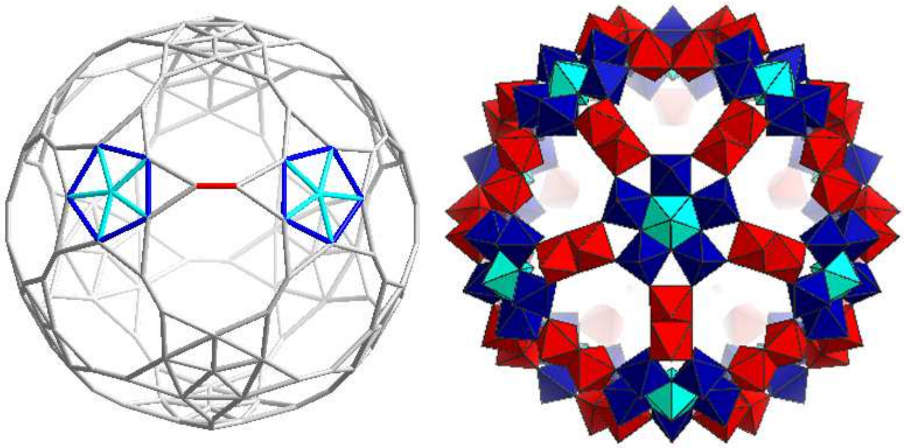

Figure 1.3: *Representations of the spherical Keplerate $\{Mo_{132}\}$ cluster. Left: schematic representation of the 132 molybdenum atom framework of the Keplerate cluster highlighting its spherical nature. Two pentagonal units, $\{(Mo)Mo_5\}$ groups, linked by an $\{Mo^V Mo^V\}$ bridge (red) are emphasized. Right: polyhedral representation of the cluster. The pentagonal Mo centers are shown by the cyan polyhedra, the rest of the $\{(Mo)Mo_5\}$ groups are shown as blue polyhedra and the $\{Mo^V Mo^V\}$ or $\{Mo_2\}$ linker groups are shown as red colored polyhedra.*

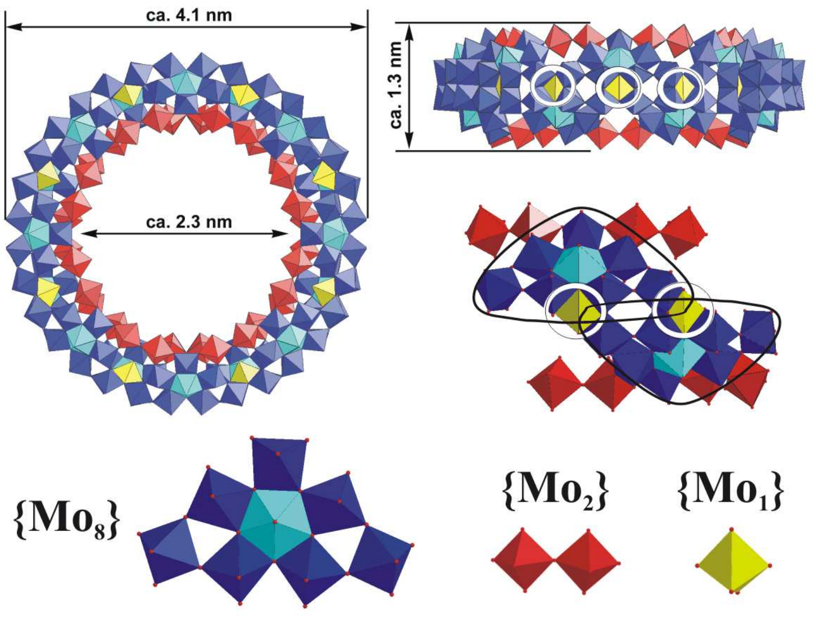

Figure 1.4: *Top (Left) and side (Right) polyhedral views of the hexameric $\{Mo-176\}$ cluster. The $\{Mo_8\}$, $\{Mo_2\}$ and $\{Mo_1\}$ building blocks are shown below and the positions of $\{Mo_1\}$ units are ringed on the side view on the Right.*

Based on the $\{Mo_8\}$-type building block very large and unusual clusters in a formal geometrical consideration are formed, including a 3.4 nm-diameter wheel-

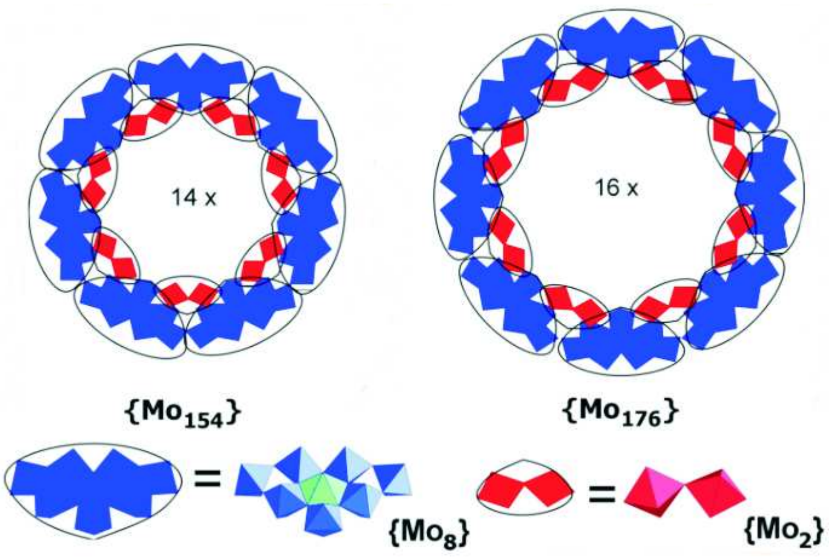

Figure 1.5: *Comparison between the* $\{Mo_{154}\}$ *and* $\{Mo_{176}\}$ *big wheel clusters. Only the top sections of the wheels are shown which comprise half of the total number of* $\{Mo_8\}$ *and* $\{Mo_2\}$ *building blocks. The equators which contain the* $\{Mo_1\}$ *building blocks are omitted for clarity along with the base of the rings which contain the other* $\{Mo_8\}$ *and* $\{Mo_2\}$ *building blocks.*

shaped metal oxide based cluster anion containing 154 molybdenum atoms, i.e. $[Mo_{154}O_{462}H_{14}(H_2O)_{70}]^{28-}$ ($\{Mo_{154}\}$) [21]. They are built up by 14 of the mentioned $\{Mo_8\}$ groups linked by 14 $\{Mo_2\}$- and 14 $\{Mo_1\}$- type units, respectively (Figure 1.2), it was metaphorically stated in New Scientist:

> ”Big wheel rolls back the molecular frontier”. [24]

An even larger ring-shaped cluster than the tetradecameric $\{Mo_{154}\}$ with 176 molybdenum atoms ($\{Mo_{176}\}$) with a 4.1 nm-diameter wheel-shaped metal-oxide based cluster anion can be obtained containing correspondingly 16 instead of 14 sets of each of the three mentioned building blocks of the type $\{Mo_8\}$, $\{Mo_2\}$ and $\{Mo_1\}$ (Figure 1.4). [12, 25]

1.3 Goals of the project: defining the problem

The work done as part of this thesis was principally oriented towards the synthesis and characterization of nanometer-scale inorganic molecules and clusters belonging to the family of polyoxomolybdates. The investigation carried out in course of this thesis revealed potential host functionalities of the ring-shaped polyoxomolybdates. Another point of interest referred to the nanosized cluster species that can be constructed as derivatives of the spherical, soluble capsules of the type $(Pentagon)_{12}(Linker)_{30}$. The robust skeleton formed exhibits 20 pores and 20 channels ending in the nanosized cavity. The chemistry is comparably easy as the basic compounds can be obtained by facile synthesis. [21] The challenge was to modify and fine-tune these anionic capsules to present different kinds of interior surfaces, pores with different sizes and chemical properties, and very importantly, different overall charges, including their effect on the interaction with small inorganic cations. The purpose was 1) to study whether this interaction takes place independent of the cavity interior shell-influence and 2) can we deliberately influence the interaction of the uptaken species by changing the internal capsule clothes. The next aim was to identify the host-potential of the capsules and to understand the dynamics of the host-guest interactions processes in (aqueous) solution. Interestingly, these capsules can be described as artificial cells and allow a new related chemistry, e.g. modeling of passive ion transport through the related inorganic membrane as well as cell response to stimuli.

Bibliography

[1] see *www.science.doe.gov/bes/scale_of_things.html* and *www.nano.gov/html /facts/The_scale_of_things.html*

[2] (a) I. V. Kozhevnikov, *Chem. Rev.*, **1998**, 98, 171; (b) N. Mizuno, M. Misono, *Chem. Rev.*, **1998**, 98, 199.

[3] (a) I. A. Weinstock, *Chem. Rev.*, **1998**, 98, 113; (b) M. Sadakane, E. Steckhan, *Chem. Rev.*, **1998**, 98, 219.

[4] T. Yamase, *Chem. Rev.*, **1998**, 98, 307.

[5] J. T. Rhule, C. L. Hill, D. A. Judd, R. F. Schinazi, *Chem. Rev.*, **1998**, 98, 327.

[6] D. E. Katsoulis, *Chem. Rev.*, **1998**, 98, 359.

[7] J. F. Keggin, *Nature*, **1933**, 131, 908.

[8] (a) M.T. Pope, A. Müller, *Angew. Chem. Int. Ed. Engl.* **1991**, 30, 34; (b) L. Cronin in *Comprehensive Coordination Chemistry II*, Vol. 7, p. 1 (Eds.-in-chief: J. A McCleverty, T. J. Meyer), Amsterdam, Elsevier, **2004**.

[9] A. Müller, E. Krickemeyer, J. Meyer, H. Bögge, F. Peters, W. Plass, E. Diemann, S. Dillinger, F. Nonnenbruch, M. Randerath, C. Menke, *Angew. Chem. Int. Ed. Engl.*, **1995**, 34, 2122.

[10] (a) A. Müller, E. Krickemeyer, H. Bögger, M. Schmidtmann, F. Peters, *Angew. Chem. Int. Ed.*, **1998**, 37, 3360; (b) A. Müller, E. Krickemeyer, H. Bögge, M. Schmidtmann, B. Botar, M. O. Talismanova, *Angew. Chem. Int. Ed.*, **2003**, 42, 2085.

[11] (a) A. Müller, E. Beckmann, H. Bögge, M. Schmidtmann, A. Dress, *Angew. Chem. Int. Ed. Engl.*, **2002**, 41, 1162; (b) A. Müller, B. Botar, S. K. Das, H. Bögge, M. Schmidtmann, A. Merca, *Polyhedron*, **2004**, 23, 2381.

[12] A. Müller, E. Krickemeyer, H. Bögge, M. Schmidtmann, C. Beugholt, P. Kögerler, C. Lu, *Angew. Chem. Int. Ed. Engl.*, **1998**, 37, 1220

[13] (a) A. Müller, S. K. Das, M. O. Talismanova, H. Bögge, P. Kögerler, M. Schmidtmann, S. S. Talismanov, M. Luban, E. Krickemeyer, *Angew. Chem. Int. Ed. Engl.*, **2002**, 41, 579.

[14] A. Müller, E. Diemann, C. Kuhlmann, W. Eimer, C. Serain, T. Tak, A. Knöchel, P. K. Pranzas, *Chem. Commun.*, **2001**, 1928.

[15] A. Müller, E. Krickemeyer, S. K. Das, P. Kögerler, S. Sarkar, H. Bögge, M. Schmidtmann, S. Sarkar, *Angew. Chem. Int. Ed. Engl.*, **2000**, 39, 1612.

[16] (a) T. Liu, *J. Am. Chem. Soc.*, **2002**, 124, 10942; (b) T. Liu, Q. Wan, Y. Xie, C. Burger, L.-Z. Liu, B. Chu, *J. Am. Chem. Soc.*, **2001**, 123, 10966; (c) T. Liu, *J. Am. Chem. Soc.*, **2003**, 125, 312.

[17] T. Liu, E. Diemann, H. Li, A. W. M. Dress, A. Müller, *Nature*, **2003**, 426, 59.

[18] A. Müller, *Science*, **2003**, 300, 749.

[19] A. Müller, C. Serain, *Acc. Chem. Res.* **2000**, 33, 2.

[20] (a) A. Müller, S. Roy, *Coord. Chem. Rev.* **2003**, 245, 153; (b) A. Müller, P. Kögerler, C. Kuhlmann, *Chem. Commun.*, **1999**, 1347.

[21] (a) L. Cronin, E. Diemann, A. Müller in *Inorganic Experiments* (Ed.: J. D. Woollins), Wiley-VCH, Weinheim, **2003**, p. 340; (b) A. Müller; S. K. Das, E. Krickemeyer, C. Kuhlmann, *Inorg. Synth.*, **2004**, 34 (Ed.: J. Shapley), p. 191.

[22] K. C. Nicolaou, E. J. Sorensen, *Classics in Total Synthesis: Targets, Strategies, Methods*, VCH, Weinheim, **1996**.

[23] H. K. Chae, W. G. Klemperer, T. A. Marquart, *Coord. Chem. Rev.*, **1993**, 128, 209.

[24] D. Bradley, *New Sci.*, November Issue, **1995**, 148, 18.

[25] A. Müller, C. Beugholt, M. Koop, S. K. Das, M. Schmidtmann, H. Bögge, *Z. Anorg. Allg. Chem.*, **1999**, 625, 1960.

[26] For a classical textbook seeI. Haiduc, The Chemistry of Inorganic Ring Systems, Vols. 1 and 2, Wiley, London, 1970.

Chapter 2

Publications

2.1 *Synergetic activation of "silent receptor" sites leading to a new type of inclusion complex: integration of a 64-membered ring comprising K^+ and SO_4^{2-} ions into a molybdenum oxide-based nanoobject*

A. Müller, *L. Toma*, H. Bögge, M. Schmidtmann and P. Kögerler

***Chem. Commun.*, 2003, 2000.**

Contribution of Liviu Toma to the following publication:

- Synthesis and characterization (electronic absorption as well as vibrational spectra, redox titration, elemental analysis) of the new compound.

COMMUNICATION

ChemComm
www.rsc.org/chemcomm

Synergetic activation of “silent receptor” sites leading to a new type of inclusion complex: integration of a 64-membered ring comprising K^+ and SO_4^{2-} ions into a molybdenum oxide-based nanoobject†‡

Achim Müller,* Liviu Toma, Hartmut Bögge, Marc Schmidtmann and Paul Kögerler
Fakultät für Chemie der Universität, Lehrstuhl für Anorganische Chemie I, Postfach 100131, D 33501 Bielefeld, Germany. E-mail: a.mueller@uni-bielefeld

Received (in Cambridge, UK) 15th May 2003, Accepted 20th June 2003
First published as an Advance Article on the web 11th July 2003

The new type of inclusion species $[Mo^{VI}_{114}Mo^{V}_{32}O_{429}(H_2O)_{50}(KSO_4)_{16}]^{30-}$ comprising 16 encapsulated K^+ and SO_4^{2-} ions shows an unusual 64-membered $\{K(SO_4)\}_{16}$ ring integrated into a wheel-shaped type nanocluster host; it is formed by a synergetically induced functional complementarity and represents a text-book example of a very complex non-biological material.

The manipulation of *well defined* objects is currently an eminent challenge in the field of nanoscience. An related task in this context is the study of cooperativity phenomena, in particular when a manifold of ingredients—as a special case also nanodots—can be positioned at equivalent sites. This cooperativity situation—formally comparable to that in extended structures showing translational invariance—can render new/important information, *e.g.* if large ring systems are considered.[1] Such rings can, in principle, also be investigated in order to extrapolate properties of infinite chains. In the present case, a suitable nanoobject is available in the form of the hexadecameric molybdenum oxide-based ring-shaped cluster of the $\{Mo_{11}\}_{16} = \{Mo_{176}\}$ type, which shows a variety of functionalities and even manifold equivalent neighbouring sites.[2] Here we report a related novel inclusion species[3] of high complexity comprising 16 integrated K^+ and SO_4^{2-} ions leading to the formation of an unusual encapsulated 64-membered ring system with distances comparable to those of solid K_2SO_4.

The nanosized system in question was obtained from a reaction mixture from which usually discrete nanosized wheel-shaped cluster species like $[Mo^{VI}_{144}Mo^{V}_{32}O_{528}H_{16}(H_2O)_{80}]^{16-} \equiv [\{Mo^{VI}_2O_5(H_2O)_2\}\{Mo^{VI/V}_8O_{26}(\mu_3\text{–}O)_2H(H_2O)_3Mo^{VI/V}\}]_{16}^{16-} \equiv [\{Mo_2\}\{Mo_8\}\{Mo_1\}]_{16}^{16-}$ **2a** are formed[2] (referred to here as $\{Mo_{176}\}$), while in presence of high K^+ and SO_4^{2-} concentrations, cluster **1a** is formed thereby integrating the corresponding ions at adjacent “receptor” type sites for anions and cations (formally considered; see below).† **1** was characterized by elemental and thermogravimetric analysis (to determine the crystal water content), cerimetric titrations [for the determination of the (formal) number of the Mo^V centers], bond valence sum (BVS) calculations (to determine the number and positions of H_2O/OH ligands as well as the formal number of Mo^V centers), spectroscopic methods (IR, resonance-Raman, Vis-NIR), EHMO calculations, and single crystal X-ray structure analysis.§ $K_{14}Na_{16}[Mo^{VI}_{114}Mo^{V}_{32}O_{429}(H_2O)_{50}\{KSO_4\}_{16}]\cdot$*ca.* 500 $H_2O \equiv K_{14}Na_{16}[\{Mo^{VI}_2O_5(H_2O)_2\}_9\{Mo^{VI/V}_8O_{24}(H_2O)_2\}_{16}\{KSO_4\}_{16}]\cdot$ *ca.* 500 H_2O **1**.

The tetragonal unit cell of **1** (space group *P* 4/*n*) shows the abundance of anionic nanosized ring-shaped units **1a**. (The defects in all $\{Mo_1\}$ and seven of the $\{Mo^{VI}\}_2$ type units occurred as usual due to increasing the pH values.†) These correspond to the parent $\{Mo_{176}\}$ type cluster **2a** and represent a new type of inclusion species (see Fig. 1). In comparison to the original $\{Mo_{176}\}$ ring the cluster anion **1a** shows the following remarkable features.

The hexadecameric parent ring system shows 16 $\{O_4\}$ tetrahedra (comparable to the well-known central $\{O_4\}$ unit of Keggin type ions, see Fig. 2) between the $\{Mo_4O_6\}$ segments encapsulating formally S^{6+} instead of H^{+2} or Cu^{2+},[4] situations already known from the completely analogous tetradecameric parent cluster $\{Mo_{11}\}_{14}$. In fact we observe, as in Keggin ions, the abundance of encapsulated SO_4^{2-} anions (S–O: 1.47–1.53 Å). Note in this context that in the central O_4 cavity of the classical Keggin ions H^+, P^{5+}, S^{6+} or M^{n+} can (formally) be correspondingly positioned.[5]

The 16 K^+ cations interact with 16 $\{Mo_6O_6\}$ crown-ether type ring systems (Fig. 2) having nucleophilic properties.[3] This interaction is supported (synergetically) by the “encapsulation” of the SO_4^{2-} anions which increases the negative charge, and thereby the nucleophilicity. To some extent referring only to the K^+ centers, a similar situation occurs for spherical nanoobjects, where *e.g.* each K^+ interacts with a slightly smaller and planar M_6O_6 type ring/pore (see ref. 6 and Fig. 1). (It was this latter fact that stimulated us to do the present type of experiment.)

The uniqueness is the presence of adjacent different specific sites, which leads to the formation and integration of an unusual

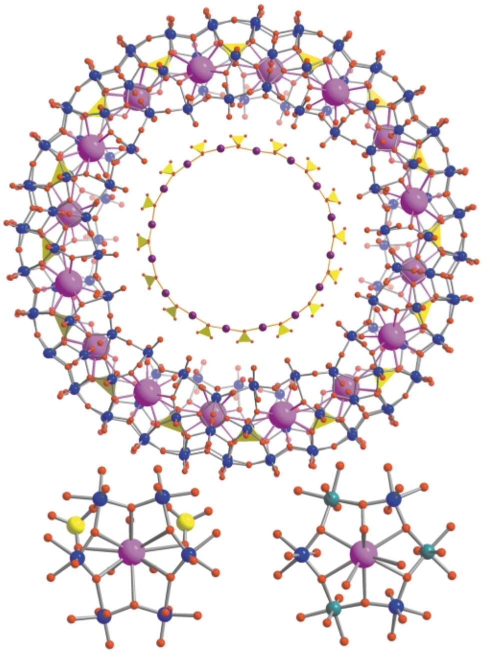

Fig. 1 Structure of **1a** in crystals of **1** in ball and stick representation but highlighting the K centers (pink spheres; for a more detailed presentation of the environment see Fig. 3) and SO_4^{2-} units (yellow; polyhedral representation). The interaction of K^+ with one $\{Mo_6O_6\}$ receptor type site in **1a** (bottom left) and the approximately comparable situation of a M_6O_6 (M = Mo, V) pore in a spherical molybdenum oxide-based system[6] (bottom right) is additionally presented. For a better demonstration of the K^+–SO_4^{2-} type interaction, the structure of the $\{K(SO_4)\}_{16}$ ring on a smaller scale and removed from its environment is shown in the center (O red, Mo blue, V/Mo turquoise).

---

† Electronic supplementary information (ESI) available: experimental and further crystallographic details. See http://www.rsc.org/suppdata/cc/b3/b305447k/

‡ Dedicated to Prof. Pierre Gouzerh on the occasion of his 60th birthday.

DOI: 10.1039/b305447k

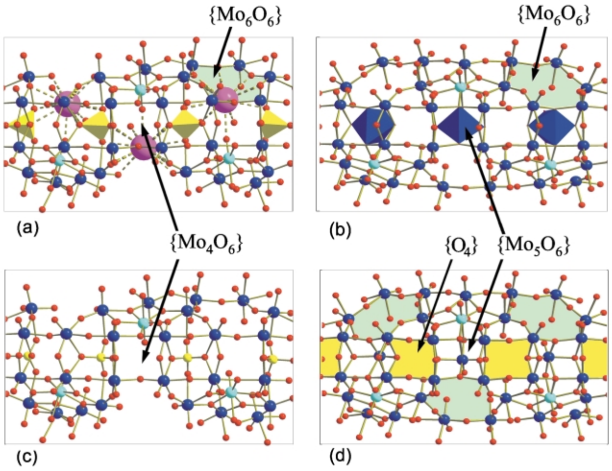

Fig. 2 Simplified demonstration of: (1) the multitude of specific adjacent "receptors" forming a zig-zag ring for K^+ ($\{Mo_6O_6\}$ rings highlighted in green) and for SO_4^{2-} ions (sites between $\{Mo_5O_6\}$ compartments schematically highlighted in yellow) (d), and (2) the change from the parent $\{Mo_2Mo_8Mo_1\}_n$ type (b, d) [2] to the $\{Mo_2\}_{n-x}\{Mo_8\}_n$ type (a, c) ring structure with the change of the $\{Mo_5O_6\}$[2] to the $\{Mo_4O_6\}$ compartments (released $\{Mo_1\}$ as blue octahedra in (b); SO_4^{2-} tetrahedra and K^+ highlighted in (a)) (colour code as in Fig. 1 with the pentagonal bipyramidal Mo type centers in cyan).

64-membered $\{KOSO\}_{16}$ type ring showing two relevant $K\cdots O$ distances of the order of 3.1 Å (Figs. 1 and 2). (The other two $K\cdots O(S)$ distances are longer.) All 16 $\{Mo_1\}$ units of the $\{Mo_5O_6\}$[2] compartments and seven $\{Mo_2\}$ building blocks of the parent $\{Mo_{176}\}$ type cluster **2a** are pushed out due to the use of the appropriate pH (for reasons see ESI†) while correspondingly 16 $\{Mo_4O_6\}$ segments are formed (Fig. 2). This has consequences for the electronic structure (as shown below). The reference to receptors is of course a simplification as the K^+ cations are also coordinated to other functions like SO_4^{2-} and to additional H_2O ligands (as shown in Fig. 3) and, correspondingly, are located *ca.* 1.5 Å below the Mo_6O_6 ring.

The IR spectrum of **1** also shows the abundance of SO_4^{2-} ions due to bands at 1176, 1118, 1043 cm^{-1}, while a comparison of the resonance Raman spectrum of the parent cluster **2a** of the type $\{Mo_{176}\}$ or $\{Mo_{154}\}$ (these are practically identical: bands at 795, 536, 462, 324, 214 cm^{-1}) with that of **1a** (793, 444, 307, 216 cm^{-1}) proves the (significant) change of the electronic structure. In both cases (*i.e.* **1a** and **2a**) the resonance Raman spectra (λ_e = 1064 nm) depend on the $Mo^V \rightarrow Mo^{VI}$ IVCT but these take place in case of **2a** within the well defined small $\{Mo_5O_6\}$ compartments.[2] The band at 536 cm^{-1} (missing in **1a**) can be tentatively assigned to a ν_s $(Mo_1(O_{br})_4)$ type vibration.

Whereas in the parent cluster **2a** two Mo-4d electrons are localized within each $\{Mo_5O_6\}$ compartment with virtually no electronic inter-compartment interactions,[7] the 32 Mo-4d electrons in **1a** are delocalized over that part of the ring system which is built up by the 16 $\{Mo_4O_6\}$ segments. Extended Hückel MO calculations† of **1a** and **2a** both reveal a set of 16 nearly degenerated molecular orbitals to form the energetically highest occupied MOs (HOMOs). These consist mostly of Mo(4d) functions of the Mo positions found in the 16 $\{Mo_4O_6\}$ segments and are separated by a significant energy gap from the lowest unoccupied MO (LUMO).[8] Compared to the parent $\{Mo_{176}\}$ cluster anion **2a**, the further delocalization of these 16 HOMOs in **1a** results in a significant decrease (*ca.* 10%) of the HOMO–LUMO gap. This decrease causes a significant increase of the temperature-independent paramagnetic contribution to the overall magnetism of **1** observed in preliminary experiments.[9,10]

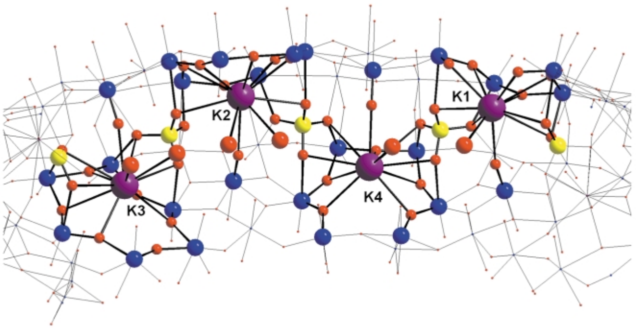

Fig. 3 Four crystallographic independent environments ($\{Mo_6O_6\}$ (or $\{Mo_4O_5\}$ in case of missing $\{Mo_2\}$ units), SO_4^{2-}, H_2O, O of $\{(Mo)Mo_5\}$) of the K^+ cations (colour code as in Fig. 1).

The present case proves that we are to some extent on the route to elucidate how reactions can be performed at non-equivalent sites of structurally *well defined* but very complex metal oxide-based nanoobjects. The related complex nanostructured landscape has a multitude of functions, *e.g.* potential "receptors" for anions and cations which have to be synergetically activated by the ions with opposite charge. This corresponds to synergetically induced functional complementarity, a situation comparable with an allosteric effect, *i.e.* the modulation of sites at distant locations due to interactions. Moreover, the present cluster system offers the potential to act polytopically for different substrates thus allowing, in principle, the study of ring-structure-based complex cooperative effects between different guests like cations and anions.

Financial support by the Deutsche Forschungsgemeinschaft, the Fonds der Chemischen Industrie, and the European Union (HPRN-CT 1999-00012) is gratefully acknowledged. L. T. thanks the Graduiertenkolleg "Strukturbildungsprozesse" of the University of Bielefeld for a fellowship.

Notes and references

§ *Crystal data* for **1a**: $H_{1100}K_{30}Mo_{146}Na_{16}O_{1043}S_{16}$, M = 33857.84 g mol^{-1}, tetragonal, space group *P*4/*n*, a = 51.726(2), c = 21.747(1) Å, V = 58185(4) $Å^3$, Z = 2, ρ = 1.933 g/cm^3, μ = 1.768 mm^{-1}, $F(000)$ = 33156, crystal size = 0.20 × 0.10 × 0.06 mm^3. Total reflections 159990 ($1.11 < \theta < 20.04°$), 27280 unique (R(int) = 0.1144). The structure was refined using SHELXL-93[11] to R = 0.0843 for 16975 reflections with $I > 2\sigma(I)$, R = 0.1427 for all reflections. CSD 412534. See http://www.rsc.org/suppdata/cc/b3/b305447k/ for crystallographic files in .cif format.

1 For a classical textbook seeI. Haiduc, *The Chemistry of Inorganic Ring Systems*, Vols. 1 and 2, Wiley, London, 1970.
2 A. Müller, P. Kögerler and C. Kuhlmann, *Chem. Commun.*, 1999, 1347–1368; A. Müller and C. Serain, *Acc. Chem. Res.*, 2000, **33**, 2–10.
3 J. W. Steed and J. L. Atwood, *Supramolecular Chemistry*, Wiley, New York, 2000; J.-M. Lehn, *Supramolecular Chemistry: Concepts and Perspectives*, VCH, Weinheim, 1995; G. A. Jeffrey, in *Inclusion Compounds*, ed. J. L. Atwood, J. E. D. Davies and D. D. MacNicol, Academic Press, New York, 1984.
4 A. Müller, E. Krickemeyer, H. Bögge, M. Schmidtmann, P. Kögerler, C. Rosu and E. Beckmann, *Angew. Chem., Int. Ed*, 2001, **40**, 4034–4037.
5 M. T. Pope and A. Müller, *Angew. Chem., Int. Ed*, 1991, **30**, 34–48.
6 A. Müller, B. Botar, H. Bögge, P. Kögerler and A. Berkle, *Chem. Commun.*, 2002, 2944–2945.
7 A typical consequence of the high degree of localization of the two Mo-centered electrons per compartment is *e.g.* the high similarity of the resonance Raman spectra of the $\{Mo_{176}\}$ and the $\{Mo_{154}\}$ type clusters and the (linear) relation between the extinction coefficient of the Mo(V) → Mo(VI) type IVCT absorption bands of molybdenum blue compounds and the formal number of Mo(V) centers.
8 This behaviour of the frontier orbitals also supports the fact that both structures **1a** and **2a** favour an electronic configuration with formally 32 Mo(V) centers.
9 P. Köyerler and A. Müller, to be published.
10 The Mulliken net charges (derived from the EHMO electronic configuration) of the molybdenum centers of the $\{Mo_4O_6\}$ segments in **1a** are non-uniform and alternate depending on their relative position with respect to the pentagonal MoO_7 bipyramids within the $\{Mo_8\}$ groups. These patterns agree well with BVS values from the corresponding single-crystal X-ray analysis.
11 SHELXS/L, G. M. Sheldrick, University of Göttingen, 1993/97.

Supplementary Material (ESI) for Chemical Communications

Synergetic activation of “silent receptor” sites leading to a new type of inclusion complex: integration of a 64-membered ring comprising K^+ and SO_4^{2-} ions into a molybdenum oxide-based nanoobject

Achim Müller,* Liviu Toma, Hartmut Bögge, Marc Schmidtmann and Paul Kögerler

Experimental details

To a solution of $Na_2MoO_4 \cdot 2\ H_2O$ (3 g, 12.4 mmol) in water (10ml) which is acidified with 0.5M H_2SO_4 (35 ml), $Na_2S_2O_4$ (0.15 g, 0.86 mmol) as reducing agent is added under stirring (immediate colour change to blue). After *ca.* 5 minutes $K_2C_2O_4$ (0.5 g) is added (to increase the pH and electrolyte concentration; CH_3COOK can be used instead) and the solution is stirred in a closed flask at about 70 ºC for 1 hour. After 5-7 days the solution is filtered and the precipitated blue crystals (mainly tetragonal prisms) are washed with cold water (50ml) (yield: 200 mg, 10% referring to molybdenum; correct analysis).

Crystal data

Crystals of **1** were removed from the mother liquor and immediately cooled to 183(2) K on a Bruker AXS SMART diffractometer (three circle goniometer with 1K CCD detector, Mo-Kα radiation, graphite monochromator; hemisphere data collection in ω at 0.3° scan width in three runs with 606, 435 and 230 frames (φ= 0, 88 and 180°) at a detector distance of 6.50 cm). A total of 159990 reflections ($1.11 < \Theta < 20.04°$) were collected of which 27280 reflections were unique (R(int) = 0.1144). An empirical absorption correction using equivalent reflections was performed with the program SADABS. The structure was solved with the program SHELXS-97 and refined using SHELXL-93 to $R = 0.0843$ for 16975 reflections with $I > 2\sigma(I)$, $R = 0.1427$ for all reflections; max./min. residual electron density 1.599 and -0.995 e Å^{-3}. (SHELXS/L, SADABS from G.M. Sheldrick, University of Göttingen, 1993/97; structure graphics with DIAMOND 2.1 from K. Brandenburg, Crystal Impact GbR, 2001.) Although the 16 K^+ positions integrated in the ring could be easily detected by the X-ray structure analysis, the number of lattice cations which are as usual disordered, had (mostly) to be determined analytically. This means that according to their relatively low abundance (*ca.* 1%), a small error limit has to be taken into account for the relative amount of Na and K.

Further details of the crystal structure determination may be obtained from the Fachinformationszentrum Karlsruhe, 76344 Eggenstein-Leopoldshafen, Germany (fax: (+49)7247-808-666; e-mail: crysdata@fiz-karlsruhe.de) on quoting the depository no. CSD 412534.

Defects in the {Mo_1} and {Mo_2} groups known from previous cases are generally observed (like in the case of the Keggin ions at relatively higher pH values [3]): see A. Müller, R. Maiti, M. Schmidtmann, H. Bögge, S. K. Das and W. Zhang, *Chem. Commun*, 2001, 2126-2127. In case of the positions where a {Mo_2} group is missing the {Mo_6O_6} "receptors" are not complete, but this has no influence on the overall structure, and especially not on the K^+ positions and the related ring formation due to the K^+-SO_4^{2-} interactions. The deep knowledge of molybdenum oxide-based systems allows to discover modifications of sphere and wheel type nanoobjects (see ref 2). Important also: the parent compounds can be obtained in facile high-yield syntheses, see A. Müller, S. K. Das, E. Krickemeyer and C. Kuhlmann, *Inorg. Synth*. 2004, **34**, in press (ed. J. Shapley).

EHMO calculations of the cluster anions **1a** and **2a** have been performed using the YAeHMOP package (G. A. Landrum and W. V. Glassey, *bind 3.0*, http://sourceforge.net/projects/yaehmop) and parameters implemented there. Proton positions of the OH and OH_2 groups were modeled to supplement the single-crystal X-ray analysis coordinates.

2.2 *Porous Capsules Allow Pore Opening and Closing That Results in Cation Uptake*

A. Müller, ***L. Toma***, H. Bögge, C. Schäffer and A. Stammler

Angew. Chem. Int. Ed., 2005, 44, 7757.

Contribution of Liviu Toma to the following publication:

- Synthesis, characterization (electronic absorption as well as vibrational spectra, redox titration, elemental analysis) and partly with help the single crystal X-ray structure analysis of the new compound **2** in the paper:

  $(H^+OC(NH_2)_2)_{15}(NH_4)_{21-n}[\{(H^+OC(NH_2)_2)_{20} + Ca_8 + (H_2O)_{60} + (NH_4)_n\}$
  $\{(Mo^{VI})Mo_5^{VI}O_{21}(H_2O)_6\}_{12}\{Mo_2^VO_4(SO_4)\}_{30}] \cdot 150H_2O$

Supramolecular Chemistry

DOI: 10.1002/anie.200502202

Porous Capsules Allow Pore Opening and Closing That Results in Cation Uptake**

Achim Müller, Liviu Toma, Hartmut Bögge, Christian Schäffer, and Anja Stammler*

Dedicated to Prof. Herbert W. Roesky
on the occasion of his 70th birthday

Structurally well-defined spherical porous molybdenum oxide based nanocapsules of the type $\{\text{Pentagon}\}_{12}\{\text{Linker}\}_{30}$[1,2] can be described as artificial cells as they allow the modeling—in solution studies—of passive biological ion transport[3a,b] as well as cell response to stimuli[3c] (see also ref. [4]); for biochemically related literature, see ref. [5a]. Specifically we refer herein to spherical, nanoscale, porous capsules/artificial cells of the type $[\{(\text{Mo})\text{Mo}_5\text{O}_{21}(\text{H}_2\text{O})_6\}_{12}\{\text{Mo}_2\text{O}_4(\text{ligand})\}_{30}]^{n-}$,[1,2] the overall charges and internal surfaces of which can be fine-tuned by changing the ligands, thus allowing the type and structure of encapsulates to be influenced.[4] Most important, the 20 $\{\text{Mo}_9\text{O}_9\}$-type pores have crown-ether-like function and can be opened and closed with noncovalently bonded guests in a supramolecular fashion.[6a] Herein we will refer to the special situation of (protonated) urea molecules as guest species,[6b] which are found in all 20 of the capsule pores. Interestingly, after exposition of a solution of this type of capsule to Ca^{2+} ions the Ca^{2+} ions are incorporated, however, in the final precipitated product all 20 pores are again closed with the urea-type guests. This situation is not only of some interest regarding modeling of cell environment interactions but fundamentally shows in an example that supramolecular chemistry is, according to J.-M. Lehn,[5b] a "dynamic chemistry/science": the interaction between the parts, that is, the capsule pores and the "corks"/guests, is based on lability, which allows an easy exchange corresponding to the reversibility of noncovalent interactions. Furthermore, we should note that "*calcium probably fulfills a greater variety of biological functions than any other cation*";[6c] this includes for instance the special role of Ca^{2+} ions in information mediation in connection with the ubiquitous presence of Ca^{2+} channels in excitable cells.[5a] In the present case, the up-taken Ca^{2+} ions influence/direct the structure of the capsule encapsulates, that is, of the water-molecule-based assembly.

Exposition of an aqueous solution of **1**[6d]—where the 20 pores are closed with protonated urea molecules—to Ca^{2+} ions leads finally to the precipitation of **2** which was characterized by elemental analysis, thermogravimetry (to determine the number of crystal water molecules), redox titration (to determine the number of Mo^{V} centers), bond valence sum (BVS) calculations,[7] spectroscopic methods (IR, Raman), and single-crystal X-ray structure analysis.[8,9]

$$\begin{aligned}&(\text{H}^+\cdot\text{OC}(\text{NH}_2)_2)_{23}(\text{NH}_4)_{29-n}[\{(\text{H}^+\cdot\text{OC}(\text{NH}_2)_2)_{20}+(\text{H}_2\text{O})_{81-n}\\&+(\text{NH}_4)_n\}\subset\{(\text{Mo}^{\text{VI}})\text{Mo}^{\text{VI}}{}_5\text{O}_{21}\,(\text{H}_2\text{O})_6\}_{12}\{\text{Mo}^{\text{V}}{}_2\text{O}_4(\text{SO}_4)\}_{30}]\cdot\\&\approx 100\,\text{H}_2\text{O}\equiv(\text{H}^+\cdot\text{OC}(\text{NH}_2)_2)_{23}(\text{NH}_4)_{29-n}\mathbf{1a}\cdot\approx 100\,\text{H}_2\text{O}\quad\mathbf{1}^{[10]}\end{aligned}$$

$$\begin{aligned}&(\text{H}^+\cdot\text{OC}(\text{NH}_2)_2)_{15}(\text{NH}_4)_{21-n}[\{(\text{H}^+\cdot\text{OC}(\text{NH}_2)_2)_{20}+\text{Ca}_8+(\text{H}_2\text{O})_{60}\\&+(\text{NH}_4)_n\}\subset\{(\text{Mo}^{\text{VI}})\ \text{Mo}^{\text{VI}}{}_5\text{O}_{21}(\text{H}_2\text{O})_6\}_{12}\{\text{Mo}^{\text{V}}{}_2\text{O}_4(\text{SO}_4)\}_{30}]\cdot\\&\approx 150\,\text{H}_2\text{O}\equiv(\text{H}^+\cdot\text{OC}(\text{NH}_2)_2)_{15}(\text{NH}_4)_{21-n}\mathbf{2a}\cdot\approx 150\,\text{H}_2\text{O}\quad\mathbf{2}\end{aligned}$$

According to the X-ray crystallographic results, the capsule **2a** (Figure 1) shows the characteristic basic polyoxomolybdate skeleton[1,2]—the artificial cell's "inorganic membrane"[4b]—that is present in **1a**,[10] and which also occurs in other spherical capsules.[1,2,4] However, in **2a** there are additionally 20 protonated urea guests closing the 20 $\{\text{Mo}_9\text{O}_9\}$ pores/rings through noncovalent (that is, hydrogen-bond) interactions[6ab], and, encapsulated Ca^{2+} ions; furthermore, the structure of the encapsulated water-molecule assembly is different in **2a** from that of **1a**. (The presence of Ca^{2+} can also be demonstrated by IR spectroscopy by the shift of a specific sulfate band from 1036 in **1** to 1057 cm^{-1} in **2**; see ref. [3a].) The eight calcium cations found in **2a** are disordered over 20 equivalent positions below the $\{\text{Mo}_9\text{O}_9\}$ pore openings at the end of the channels (Figure 1), that is, on the C_3 axes, and exhibit the expected octahedral coordination environment which is formed by three oxygen atoms of three sulfate ligands and three oxygen atoms belonging to the encapsulated water shell/assembly (see below and ref. [4]). Whereas **1a** shows the known structure of the $\text{NH}_4{}^+/\text{H}_2\text{O}$ assembly within a capsule containing $\text{SO}_4{}^{2-}$ ligands,[4a] in **2a** a

---

[*] Prof. Dr. A. Müller, L. Toma, Dr. H. Bögge, C. Schäffer, A. Stammler
Lehrstuhl für Anorganische Chemie I
Fakultät für Chemie der Universität
Postfach 100131, 33501 Bielefeld (Germany)
Fax: (+49) 521-106-6003
E-mail: a.mueller@uni-bielefeld.de

[**] Financial support from the Deutsche Forschungsgemeinschaft, the Fonds der Chemischen Industrie, the Volkswagenstiftung, the German–Israeli Foundation for Scientific Research and Development (GIF), and the European Union is gratefully acknowledged. L.T. thanks the Graduiertenkolleg "Strukturbildungsprozesse" of the University of Bielefeld for a fellowship. Furthermore, the contributions from Dr. Alice Merca and Dr. Soumyajit Roy (preparation of the educt) as well as Dr. Andreas Mix (NMR spectra) are acknowledged.

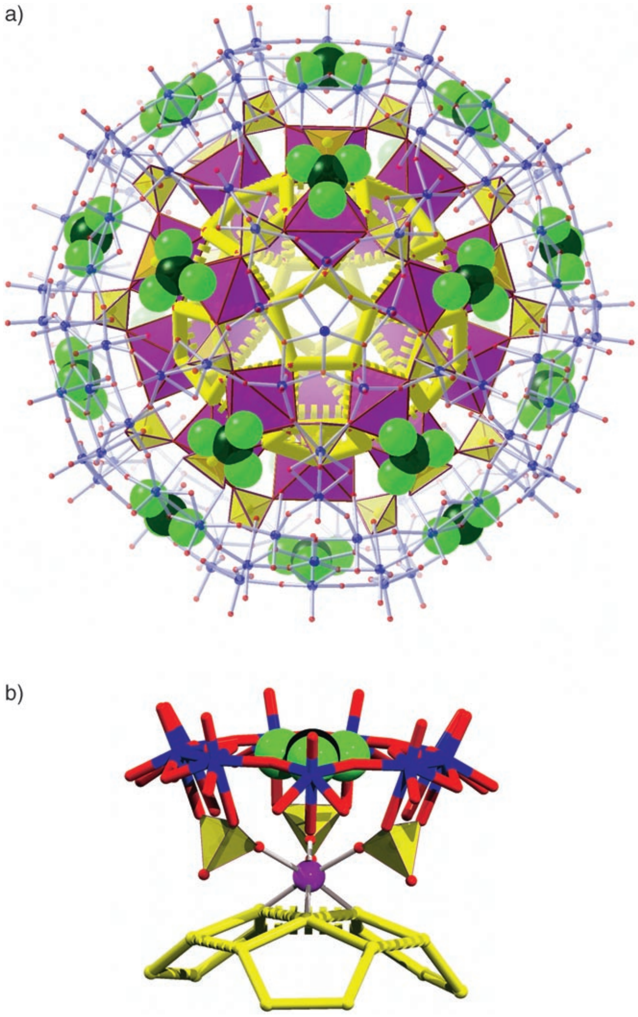

Figure 1. a) Structure of the capsule **2a** with the skeleton in ball-and-stick representation (Mo blue, O red), sulfate ligands (yellow tetrahedra), Ca^{2+} ions in the octahedral coordination of oxygen atoms (pink octahedra), the rhombicosidodecahedral $(H_2O)_{60}$ water assembly inside the capsule (yellow wire-frame representation, solid and dotted lines), and the protonated urea corks (space-filling representation, C dark green, N/O (urea) green). b) For clarity one segment of **2a** is shown separately (same color code as in (a)).

pure, well-defined water assembly/shell $\{H_2O\}_{60} \approx 12\{H_2O\}_5$ (radius 6.81–7.12 Å; occupation factor 1 for the O atoms) acting as ligand to the Ca^{2+} ions is observed,[11a] the formation and positioning of which is directed by the abundance of the fixed Ca^{2+} ions. (Though the exact NH_4^+ and H_2O positions in **1a** cannot be distinguished by X-ray crystallography because of a related disorder, there is clear evidence that NH_4^+ ions are involved in the formation of the central $\{X_{20}\}$ dodecahedron.[11a]) The $(H_2O)_{60}$ shell of **2a** corresponds to a distorted rhombicosidodecahedron which might be regarded as an unprecedented polydentate/macrocyclic ligand for the calcium ions or other cations.

Recall that we start with a capsule **1a** closed by the protonated urea "corks" and detect Ca^{2+} ions afterwards in the capsule **2a**, the pores of which are again closed by the same corks. The inorganic membrane pores are definitely not permanently closed, and in solution only a fraction of the pores is always (statistically) open (Figure 2). This problem related to the "behavior" of the corks in solution cannot of course be solved by an X-ray crystallography study. On the other hand, preliminary ^1H NMR spectra of solutions of **2** in DMF at room temperature clearly indicate the abundance of oxygen-protonated urea species in the pores.[11b] (Oxygen protonation would agree with earlier results for the protonation sites of urea determined by IR and ^{17}O NMR spectroscopy.[6b]) In this case, the peak-intensity analysis reveals that approximately a third of the capsule pores are occupied.[11c] Interesting, in this context, is the possibility of stabilizing the OH-type protonated urea species by integration into the pores. Furthermore, a well-defined temperature-dependent equilibrium can—in the case of guest cations exhibiting a much higher affinity[6a] for the pores than protonated urea—be easily studied by NMR spectroscopy in different solvents.[11d] With such guests the remarkable situation arises in which all the 20 pores are completely closed at lower temperatures and can be (reversibly) opened on heating with the consequence that uptake of different types of cations only occurs at higher temperatures (temperature gating). This process can be demonstrated nicely by ^1H- and metal-NMR spectroscopy studies including EXSY data.[11d]

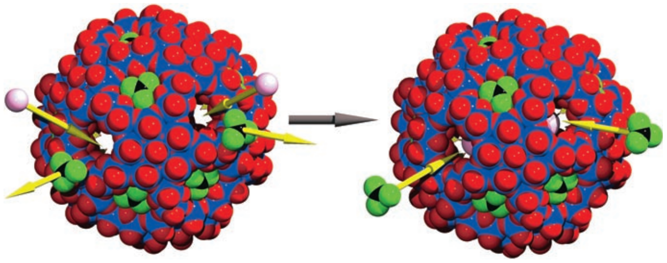

Figure 2. Space-filling representation demonstrating a simplified view of the Ca^{2+} ion uptake based on the capsule **1a**. In the anions of **1** the pores are closed. Treating a solution of **1** with Ca^{2+} ions leads to cation uptake (left) while in the final product **2** the pores again are closed (right; Mo blue, O red, C black, N/O(urea) green, Ca^{2+} pink, yellow arrows indicate direction of motion).

Under the conditions employed the Ca^{2+} ions cannot pass through the pores with their hydrate coat: for an effective trafficking the comparably large Ca^{2+} complexes must release their water ligands and some of these ligands are "taken up" again inside the artificial cell. (Note: the inorganic membrane pores are semipermeable allowing uptake and release of water but not of organic solvents such as DMF or DMSO.[3b,11d]) A condition for the uptake is therefore that the affinity of Ca^{2+} ions for the H_2O ligands is not too strong. This condition is met in this case as the water ligand "mean residence time" is of the order around 10^{-8} s at room temperature,[12] which is comparable to the published water exchange rate constant of $6–9{\cdot}10^8\ s^{-1}$.[13ab,14] As $[Ca(H_2O)_6]^{2+}$ shows a much greater lability compared to the related Be^{2+} and Mg^{2+} hydrate complexes, Be^{2+} and Mg^{2+} should therefore both show a different behavior with respect to their interactions with the capsule(s).[14] In this context there is another attractive aspect which is related to the possibility of trapping complete hydrate complexes above the capsules' pores based on hydrogen-bond interactions between the O atoms of the $\{Mo_9O_9\}$ pores/rings and the H_2O ligands. But this type of trapping only occurs for the present type of hydrate complex, which has a low stability-constant value, with less negatively charged capsules, for example, those with linkers containing less negatively charged ligands, such as acetates (instead of sulfates), where the capsule–cation interaction is weaker.[15] Interesting in this context is that the coordination environment of calcium ions in water is not very well defined, and correspondingly different coordination numbers for Ca^{2+} ions are reported in the literature.[13a] This gives, in principle, the option to trap different hydrate complexes in this or in related metal complexes at the capsule surface sites under different conditions,[13c] including different capsule charges (so called "Sphere Surface Chemistry").

An aspect of more general interest in this context is the chance to carry out systematic studies on the interaction between the capsules/artificial cells—the pores of which are partially or temporarily closed with different kinds of complementary guests—and a series of different hydrated cations present in solution; this would allow information to be obtained on the properties and behavior of hydrate complexes. The entrance of appropriate cations can nicely be studied in solution with NMR spectroscopy.[3a,b] Importantly, most of the biological ion pores/channels are not continuously open (note: the K^+ ion leak channels are) they are gated, that is, they can open and then close again.[5a] The opening is due to a response to specific stimuli, for example, corresponding to a change in the voltage across the membrane (leading to the channel protein conformational changes), a mechanical stress, or binding of a ligand.[5a] Referring to the present situation, the abundance of a large number of added cations, such as Ca^{2+}, in the vicinity or at the surface of the highly charged capsule decreases the capsule's charge, that is, diminishes the formal electrochemical gradient.[5a] This can 1) facilitate the release of guests such as protonated (even comparably strongly bonded) organic bases complementary to the $\{Mo_9O_9\}$ pores, and 2) allow subsequent entering of the cations (voltage gating of channels[5a]). In the case of more strongly bonded guests (see above and ref. [6]), this leads to complete pore closing at lower temperatures and cation uptake is observed only at higher temperatures (temperature gating (see above)). Once the cations are encapsulated the charge distribution changes, which might again influence the gating of the pores.

In the present system cation entrance is interesting because of the following facts: Voltage-gated calcium channels—ubiquitous in excitable cells in which Ca^{2+} functions as the ubiquitous intracellular messenger—play a key role in various physiological processes, such as muscle contraction, hormone and neurotransmitter secretion, and neuronal excitability. Several extracellular signals can induce an increase in the cytosolic Ca^{2+} ion concentration by 10–20-fold, which triggers the response.[5a,16,17] An interesting result of the present study is also that the uptake of Ca^{2+} ions leads to a "response in the cavity" in the form of a change in the structure of the encapsulates, that is, of the water/electrolyte based assembly.

Experimental Section

Synthesis of **1** (see also ref. [10]): A mixture of $(NH_4)_{42}[\{(Mo)Mo_5O_{21}(H_2O)_6\}_{12}\{Mo_2O_4(CH_3COO)\}_{30}]\cdot\approx[10\,CH_3COONH_4+300\,H_2O]$ (1.0 g, 0.04 mmol),[2d] ammonium sulfate (4.0 g, 30 mmol), urea (3.0 g, 50 mmol), and water (100 mL) was acidified with 16% HCl (8 mL) in a 250-mL conical flask (covered with a watch-glass) and stirred for 45 min at room temperature. The solution was kept in an open 250-mL beaker at around 23 °C for 10 days. Then the precipitated brown rhombohedral crystals of **1** were collected by filtration and dried in air. Yield: 0.35 g (35% based on Mo); elemental analyses (%) calcd N 5.69, H 2.62, C 1.82; found: N 5.6, H 2.7, C 1.8.

Characteristic IR bands: (KBr pellet, some characteristic bands for the range 1700–500 cm^{-1}): $\tilde{\nu}=1703$ [w, $\delta(ureaH^+)$], 1622 [s, $\delta(H_2O)$], 1555 [w, $\delta(ureaH^+)$], 1402 [m, $\delta(NH_4)$], 1196 (w), 1140 (m), 1036 (w) [all $\nu_{as}(SO_4)$], 972 [s, $\nu(Mo{=}O)$], 852 (m), 795 (s), 723 (s), 630 (w), 569 cm^{-1} (s). (The $ureaH^+$ bands are influenced by the hydrogen bonds in the pores and are rather different from those of urea itself.)

Characteristic Raman bands: (solid state, KBr dilution, $\lambda_e\approx1064$ nm): $\tilde{\nu}=950$ [m, $\nu(Mo{=}O)$], 880 [ν_s ($O_{bridging}$ breathing/A_{1g})], 372 (m), 303 cm^{-1} (w).

2: A mixture of **1** (2.0 g, 0.07 mmol), $CaCl_2\cdot2H_2O$ (0.5 g, 3.40 mmol), and water (50 mL; pH < 2) was stirred for 2 h at room temperature. The solution was then kept in an open 250-mL beaker at about 23 °C and after one week the precipitated brown rhombohedral crystals were collected by filtration through a glass frit (D2) and dried in air. Yield: 0.6 g (30% based on Mo); elemental analyses (%) calcd N 4.47, C 1.47, H 2.55, Ca 1.12; found: N 4.5, C 1.5, H 2.4, Ca 1.1.

Characteristic IR bands: (KBr pellet, some characteristic bands for the range 1700–500 cm^{-1}): $\tilde{\nu}=1703$ [w, $\delta(ureaH^+)$], 1624 [s, $\delta(H_2O)$], 1555 [w, $\delta(ureaH^+)$], 1402 [s, $\delta(NH_4)$], ≈1200 (sh), 1143 (m-s), 1057 (w) [all $\nu_{as}(SO_4)$], 976 (s), 947 (w) [both $\nu(Mo{=}O)$], 854 (m), 796 (s), 725 (s), 632 (w), 573 cm^{-1} (s).

Characteristic Raman bands: (solid state, KBr dilution, $\lambda_e\approx1064$ nm): $\tilde{\nu}=950$ [m, $\nu(Mo{=}O)$], 879 [ν_s ($O_{bridging}$ breathing/A_{1g})], 372 (m), 302 cm^{-1} (w).

The chemical formulae of **1** and **2** refer to the maximum possible number of crystal water molecules which correspond to the related volume calculated from the cell volume and the sum of volumes of all cell ingredients excluding those of the crystal water molecules. The given calculated values for C, N, Ca are related to a formula with 50 crystal water molecules less than given (note: **1** and **2** as all similar compounds show slow weathering, that is, loss of crystal water).

Received: June 23, 2005

Keywords: calcium · ion transport · molybdenum · polyoxometalates · porous capsules

---

[1] L. Cronin in *Comprehensive Coordination Chemistry II, Vol. 7* (Eds.: J. A. McCleverty, T. J. Meyer), Elsevier, Amsterdam, **2004**, pp. 1–56.

[2] a) A. Müller, P. Kögerler, C. Kuhlmann, *Chem. Commun.* **1999**, 1347–1358; b) A. Müller, S. Roy, *Coord. Chem. Rev.* **2003**, *245*, 153–166; c) L. Cronin, E. Diemann, A. Müller in *Inorganic Experiments*, 2nd ed. (Ed.: J. D. Woollins), Wiley-VCH, Weinheim, **2003**, pp. 340–346; d) A. Müller, S. K. Das, E. Krickemeyer, C. Kuhlmann, *Inorg. Synth.* (Ed.: J. R. Shapley) **2004**, *34*, pp. 191–200; e) A. Müller, S. Roy in *The Chemistry of Nanomaterials: Synthesis, Properties and Applications* (Eds.: C. N. R. Rao, A. Müller, A. K. Cheetham), Wiley-VCH, Wein-

heim, **2004**, pp. 452–475; f) N. Hall, *Chem. Commun.* **2003**, 803–806.

[3] This finding is based on ^{7}Li NMR solution studies: a) A. Müller, D. Rehder, E. T. K. Haupt, A. Merca, H. Bögge, M. Schmidtmann, G. Heinze-Brückner, *Angew. Chem.* **2004**, *116*, 4566–4570; *Angew. Chem. Int. Ed.* **2004**, *43*, 4466–4470; corrigendum: A. Müller, D. Rehder, E. T. K. Haupt, A. Merca, H. Bögge, M. Schmidtmann, G. Heinze-Brückner, *Angew. Chem.* **2004**, *116*, 5225; *Angew. Chem. Int. Ed.* **2004**, *43*, 43, 5115 (see also: M. Gross, *Chem. World* **2004**, *1*, 18) and; b) E. T. K. Haupt, C. Wontorra, D. Rehder, A. Müller, *Chem. Commun.* **2005**, 3912–3914; c) A. Müller, E. Krickemeyer, H. Bögge, M. Schmidtmann, S. Roy, A. Berkle, *Angew. Chem.* **2002**, *114*, 3756–3761; *Angew. Chem. Int. Ed.* **2002**, *41*, 3604–3609.

[4] a) A. Müller, E. Krickemeyer, H. Bögge, M. Schmidtmann, B. Botar, M. O. Talismanova, *Angew. Chem.* **2003**, *115*, 2131–2136; *Angew. Chem. Int. Ed.* **2003**, *42*, 2085–2090; b) A. Müller, H. Bögge, M. Henry, *C. R. Chim.* **2005**, *8*, 47–56; c) M. Henry, H. Bögge, E. Diemann, A. Müller, *J. Mol. Liq.* **2005**, *118*, 155–162; d) A. Müller, S. K. Das, S. Talismanov, S. Roy, E. Beckmann, H. Bögge, M. Schmidtmann, A. Merca, A. Berkle, L. Allouche, Y. Zhou, L. Zhang, *Angew. Chem.* **2003**, *115*, 5139–5198; *Angew. Chem. Int. Ed.* **2003**, *42*, 5039–5044.

[5] a) B. Alberts, A. Johnson, J. Lewis, M. Raff, K. Roberts, P. Walter, *Molecular Biology of the Cell*, 4th ed., Garland Science, New York, **2002**; b) J.-M. Lehn, *Proc. Natl. Acad. Sci. USA* **2002**, *99*, 4763–4768, and references therein.

[6] a) The first published example referred to the integration of $20[C(NH_2)_3]^+$ ions into the $20\{Mo_9O_9\}$ pores/rings in the same way as into a crown ether host, that is, the O···H–N bonding is comparable to that in crown ether hosts; for details see ref. [3c]. The pore(host)–guest interactions with other protonated bases such as $H^+{\cdot}OC(NH_2)_2$ (see below) and $HC(NH_2)_2^+$ (unpublished results; see also comments in the text) are as expected weaker, while with the increasing basicity of the corresponding unprotonated base—which is lowest in case of urea—the stability of the protonated species increases (H. R. Christen, F. Vögtle, *Organische Chemie, Vol. 1*, Salle and Sauerländer, Frankfurt am Main, **1992**, p. 452); b) Urea is, apart from its biological (e.g., protein denaturation) and industrial importance (see, for example, J. W. Steed, J. L. Atwood, *Supramolecular Chemistry*, Wiley, New York, **2000**, p. 273), especially interesting structurally and chemically: firstly because of the abundance of the (complementary) hydrogen-bonding sites giving rise to the remarkable cage/inclusion structures (see, for example, G. A. Jeffrey, *An Introduction to Hydrogen Bonding*, Oxford University Press, New York, **1997**, p. 175), and secondly to the (in principle) different sites for protonation, that is, at the N and O atoms. The OH type species is stabilized by the contribution of the mesomeric border structure exhibiting the $C{=}NH_2^+$ fragment (K. P. C. Vollhardt, N. E. Schore, *Organische Chemie*, Wiley-VCH, 3. Aufl, Weinheim, **2000**, p. 956; see also: H. Beyer, W. Walter, *Lehrbuch der Organischen Chemie*, Hirzel, Stuttgart, 21. Aufl., **1988**, p. 356). Important in this case is that O protonation allows hydrogen-bond interactions in the pores in three directions. The problem of protonated sites was controversial for a long time starting from Alfred Werner's opinion: From vibrational spectra of normal urea salts, for example, with the $PtCl_6^{2-}$ ion, it was concluded for the first time that the preferable site of protonation is the O atom (W. Kutzelnigg, R. Mecke, *Chem. Ber.* **1961**, *94*, 1706–1716). Also from ^{17}O NMR spectroscopy studies over a wide pH range, from aqueous solution to fluoro sulfonic acid, it was concluded that (the first) protonation takes place at the O atom; in a magic acid even double protonation was observed (B. Valentine, T. E. St. Amour, D. Fiat, *Org. Magn. Reson.* **1984**, *22*, 697–700); c) W. Kaim, B. Schwederski, *Bioinorganic Chemistry: Inorganic Elements in the Chemistry of Life*, Wiley, Chichester, **1994**, p. 293; d) Note: this type of capsules is stable in solution at pH values between 1.5 and 4 and under exclusion of oxygen.

[7] I. D. Brown in *Structure and Bonding in Crystals, Vol. II* (Eds.: M. O'Keeffe, A. Navrotsky), Academic Press, New York, **1981**, pp. 1–30.

[8] Crystal data for **2**: $C_{35}H_{823}Ca_8Mo_{132}N_{91}O_{809}S_{30}$, $M_r = 29\,415.4$ g mol^{-1}, rhombohedral, space group $R\bar{3}$, $a = 32.8169(7)$, $c = 73.921(2)$ Å, $V = 68\,944(3)$ Å^3, $Z = 3$, $\rho = 2.125$ g cm^{-3}, $\mu = 1.96$ mm^{-1}, $F(000) = 42\,978$, crystal size $= 0.40 \times 0.30 \times 0.30$ mm^3. Crystals of **2** were removed from the mother liquor and immediately cooled to 183(2) K on a Bruker AXS SMART diffractometer (three circle goniometer with 1 K CCD detector, $Mo_{K\alpha}$ radiation, graphite monochromator; hemisphere data collection in ω at 0.3° scan width in three runs with 606, 435, and 230 frames ($\varphi = 0$, 88 and 180°) at a detector distance of 5.00 cm). A total of 115 162 reflections ($1.55 < \Theta < 27.01°$) were collected of which 32 366 reflections were unique ($R(\text{int}) = 0.0290$). An empirical absorption correction using equivalent reflections was performed with the program SADABS 2.10. The structure was solved with the program SHELXS-97 and refined using SHELXL-97 to $R = 0.0389$ for 27 502 reflections with $I > 2\sigma(I)$, $R = 0.0487$ for all reflections; max./min. residual electron density 1.87 and -1.85 e Å^{-3} (SHELXS/L, SADABS from G. M. Sheldrick, University of Göttingen, **1997/2003**; structure graphics with DIAMOND 3.0, http://www.crystalimpact.com/ and with POV-Ray 3.6, http://www.povray.org/).

[9] The basic structure of the educt **1**[10], for which the synthesis is also given (see Experimental Section), corresponds to that of **2**.

[10] a) S. Roy, Thesis, Faculty of Chemistry, University of Bielefeld, **2005**; b) A. Müller, A. Merca, S. Roy, H. Bögge, M. Schmidtmann, unpublished results.

[11] a) The shell system in the cavity of **1a** spanned by $n\,NH_4^+/m\,H_2O = X$ centers with $m \geqslant n$ is X_{60} (distorted rhombicosidodecahedron) + X_{20} (dodecahedron) + X (in the center) and is also found, for example, in an ammonium/sulfate-based capsule with open pores;[4a] the X_{60} shell is geometrically similar to the known pure water assembly $\{H_2O\}_{60}$ shell such as that in **2a** (see also ref. [4b,c]). There is clear evidence that the NH_4^+ ions in **1a** are rather strongly fixed in the cavity, as shown by combined thermogravimetry, mass spectroscopy, and temperature-dependent elemental analyses studies up to 450 °C; remarkably, the release of the "last" NH_3 molecules out of the capsules upon heating occurs at rather high temperatures (A. Malecki, A. Bielanski, E. Diemann, A. Müller, unpublished results). On the other hand it is evident that a change of the positions of the NH_4^+ ions during the conversion of **1a** into **2a** occurs while a Ca^{2+}–NH_4^+ counter transport takes place which leads to very small values of n in **2** and is currently being investigated in detail by ^{15}N HSQC NMR spectroscopy (E. T. K. Haupt, A. Müller, unpublished results); b) A. Mix, H. Bögge, T. Mitra, D. Rehder, A. Müller, unpublished results; c) In an aqueous solution of **1** the ratio of open to closed pores is unknown. The complete pore closing observed in solid **2** is to some extent influenced by the fact that it lowers the capsule charge and leads to a lower solubility of **2**; d) A. Mix, H. Bögge, D. Rehder, T. Mitra, M. Schmidtmann, A. Müller, unpublished results.

[12] F. A. Cotton, G. Wilkinson, C. A. Murillo, M. Bochmann, *Advanced Inorganic Chemistry*, 6th ed., Wiley, New York, **1999**, page 59.

[13] a) D. T. Richens, *The Chemistry of Aqua Ions: Synthesis, Structure and Reactivity: A Tour Through the Periodic Table of the Elements*, Wiley, Chichester, **1997**; b) See also: H. Krüger, *Chem. Soc. Rev.* **1982**, *11*, 227–256; c) Regarding unprecedented coordination numbers it should be mentioned in this context that recently for the first time evidence for a fivefold coordination of a trivalent metal aqua ion, that is, of Al^{III} could be obtained

(T. W. Swaddle, J. Rosenqvist, P. Yu, E. Bylaska, B. L. Phillips, W. H. Casey, *Science* **2005**, *308*, 1450–1453).

[14] The exchange rate for water ligands in the Ca^{2+} complex is, for instance, too fast to be measured by dynamic NMR spectroscopy.[13]

[15] A. Müller, L. Toma, H. Bögge, M. Schmidtmann unpublished results; see also Ref. [4b].

[16] a) B. Hille, *Ion Channels of Excitable Membranes*, 3rd ed., Sinauer, Massachusetts, **2001**; b) D. E. Clapham, *Nature* **2003**, *426*, 517–524.

[17] The surface of the excitable cell type mentioned holds thousands of related channels that precisely control the timing and entry of Ca^{2+} ions. Furthermore, the inhibition of the Ca^{2+} ion entry through channels by antagonists/entry blockers is of tremendous importance for the treatment of hypertony and coronary heart diseases because an excess of Ca^{2+} ions in the cells has to be avoided, a situation which nature can normally remedy through an effective control by Ca^{2+} ion pumps (T. A. Scott, E. I. Mercer, *Concise Encyclopedia Biochemistry and Molecular Biology*, 3rd ed., de Gruyter, New York, **1997**; E. Mutschler, *Arzneimittelwirkungen*, Wissenschaftliche Verlagsgesellschaft, Stuttgart, **1986**, p. 447).

2.3 *Reactions inside a porous nanocapsule/artificial cell: encapsulates' structuring directed by internal surface deprotonations*

A. Müller, *L. Toma*, H. Bögge, M. Henry, E. T. K. Haupt, A. Mix and F. L. Sousa

***Chem. Commun.*, 2006, 3396.**

Contribution of Liviu Toma to the following publication:

- Synthesis, characterization (electronic absorption as well as vibrational spectra, redox titration, elemental analysis) and partly with help the single crystal X-ray structure analysis of the new compounds.

Reactions inside a porous nanocapsule/artificial cell: encapsulates' structuring directed by internal surface deprotonations†‡

Achim Müller,*[a] Liviu Toma,[a] Hartmut Bögge,[a] Marc Henry,[b] Erhard T. K. Haupt,[c] Andreas Mix[a] and Filipa L. Sousa[a]

Received (in Cambridge, UK) 28th March 2006, Accepted 13th June 2006
First published as an Advance Article on the web 5th July 2006
DOI: 10.1039/b604557j

In the cavities of unprecedentedly functionalised, spherical, porous capsules of the type $\{\text{Pentagon}\}_{12}\{\text{Linker}\}_{30} \equiv [\{(\text{Mo})\text{Mo}_5\text{O}_{21}(\text{H}_2\text{O})_6\}_{12}\{\text{Mo}_2\text{O}_4(\text{ligand})\}_{30}]^{n-}$ reactions with the ligands – *i.e.* at the internal shell surfaces – can be performed, in the present case deliberate aquation/hydration and deprotonation reactions at the linker fragments $\{(\text{Mo}_2\text{O}_4)\text{C}_2\text{O}_4\text{H}\}^+$ similar to that reported in the literature for $[(\text{NH}_3)_5\text{CoC}_2\text{O}_4\text{H}]^{2+}$ in solution.

Generally speaking, what is it like for molecules to be 'housed' inside a nanosized molecular capsule, *i.e.* under confined conditions, with respect to interactions between themselves? Can these interactions take place (nearly) independently from the cavity-interior shell-functionalities – as in a test-tube – or is there the option to influence deliberately the interactions of uptaken molecules by tuning appropriately the internal capsule functionalities? These questions can be addressed now as it is possible to fine-tune the functionalities – from rather inert to strongly directing – of the interior surface of soluble, spherical, porous capsules of the type $\{\text{Pentagon}\}_{12}\{\text{Linker}\}_{30} \equiv [\{(\text{Mo})\text{Mo}_5\text{O}_{21}(\text{H}_2\text{O})_6\}_{12}\{\text{Mo}_2\text{O}_4(\text{ligand})\}_{30}]^{n-}$ (for ligand = acetate with $n = 42$ this corresponds to the educt **1a**).[1–5] Modifications of the cluster interiors can be carried out by exchanging the ligands coordinated to the 30 $\{\text{Mo}_2\}$ linkers, in the present case by substituting 30 acetate ligands existing in the easily obtained compound **1**,[4] by 30 monoprotonated oxalate ligands. In the resulting compound **2** internal surface reactions, *i.e.* aquations (oxalate–water exchange) and deprotonations were performed. This leads to **3**, demonstrating that the deprotonations direct the structuring of the encapsulated $\text{H}_2\text{O}/\text{NH}_4^+$ assemblies.

$(\text{NH}_4)_{42}[\{(\text{Mo}^{\text{VI}})\text{Mo}^{\text{VI}}_5\text{O}_{21}(\text{H}_2\text{O})_6\}_{12}\{\text{Mo}^{\text{V}}_2\text{O}_4(\text{OOCCH}_3)\}_{30}]\cdot ca.\{300\text{H}_2\text{O} + 10\text{CH}_3\text{COONH}_4\} \equiv (\text{NH}_4)_{42}\cdot$**1a**$\cdot$lattice ingredients $\equiv$ **1**.

$(\text{NH}_4)_{42}[\{(\text{Mo}^{\text{VI}})\text{Mo}^{\text{VI}}_5\text{O}_{21}(\text{H}_2\text{O})_6\}_{12}\{\text{Mo}^{\text{V}}_2\text{O}_4(\text{OOCCOOH})\}_{30}]\cdot ca.\{300\text{H}_2\text{O} + 2\text{C}_2\text{H}_2\text{O}_4\} \equiv (\text{NH}_4)_{42}\cdot$**2a**$\cdot$lattice ingredients $\equiv$ **2**.

$(\text{NH}_4)_{38}[\{(\text{H}_2\text{O})_x + (\text{NH}_4)_{14}\}\subset\{(\text{Mo}^{\text{VI}})\text{Mo}^{\text{VI}}_5\text{O}_{21}(\text{H}_2\text{O})_6\}_{12}\{\text{Mo}^{\text{V}}_2\text{O}_4(\text{OOCCOOH})\}_8\{\text{Mo}^{\text{V}}_2\text{O}_4(\text{OOCCOO})\}_{16}\{\text{Mo}^{\text{V}}_2\text{O}_4(\text{H}_2\text{O})_2\}_6]\cdot ca.(300 - x)\text{H}_2\text{O} \equiv (\text{NH}_4)_{36}\cdot$**3a**$\cdot ca.(300 - x)\text{H}_2\text{O} \equiv$ **3**.

By reaction of an aqueous solution of **1** with oxalic acid§ compound **2** was obtained. Afterwards, **2** was dissolved in water to initiate ligand based reactions, *i.e.* aquations/hydrations and deprotonations, which led to compound **3** containing structured encapsulates not present in **2**.¶ Compounds **2** and **3** were characterised by elemental analysis, thermogravimetry (to determine the number of crystal water molecules), redox titration (to determine the number of Mo^{V} centres), bond valence sum (BVS) calculations,[6a] spectroscopically (NMR, IR, Raman), and by single crystal X-ray structure analysis.‖

The capsules **2a** and **3a** exhibit the above mentioned "classical" spherical polyoxomolybdate skeleton found in **1** and in several other related compounds (Fig. 1).[1–5] Whereas **2a** shows at the 30 equivalent linker positions 30 identical monoprotonated oxalate ligands, **3a** shows unprecedented internal structural features¶ as a result of reactions at the internal cavity surface. The detailed interpretation of the single crystal X-ray structure and the elemental analysis of **3**‖ proves the presence of (i) 24 partially deprotonated ligands distributed statistically over the related 30 positions, *i.e.* coordinated to the $\{\text{Mo}_2\}$ type linkers, and (ii) six binuclear linkers $\{\text{Mo}_2\}$ carrying two water molecules as ligands (see formula). Hence, six monoprotonated oxalate ligands are replaced due to aquation/hydration reactions (Fig. 2). This ligand exchange $\{(\text{Mo}_2\text{O}_4)\text{C}_2\text{O}_4\text{H}\}^+ \rightarrow \{(\text{Mo}_2\text{O}_4)(\text{H}_2\text{O})_2\}^{2+}$ favours deprotonation§ due to the corresponding decrease of the overall negative cluster charge. In **2a** the ligands are not deprotonated, as **2** is formed in the presence of an excess of oxalic acid.§ But the deprotonation of **2a** – resulting in the

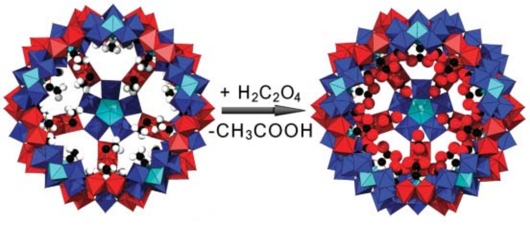

Fig. 1 Schematic demonstration of how the inner surface of the porous spherical nanocapsule **1a** changes on replacing acetate (left) by oxalate ligands (right). For clarity, one pentagonal unit and five linkers are omitted ($\{(\text{Mo})\text{Mo}_5\}$ units (blue/cyan), $\{\text{Mo}^{\text{V}}_2\}$ type linkers (red) in polyhedral representation, C black, H white). Right: corresponding hydrophilic inner capsule surface in **2a** without H atoms.

---

[a] *Fakultät für Chemie der Universität, Postfach 100131, 33501, Bielefeld, Germany. E-mail: a.mueller@uni-bielefeld.de*
[b] *NMR and Solid State Molecular Chemistry, Université Louis Pasteur, Institut Le Bel, 4 Rue Blaise Pascal, 67070, Strasbourg, France*
[c] *Institut für Anorganische und Angewandte Chemie der Universität, 20146, Hamburg, Germany*

† Dedicated to Professor F. A. Cotton on the occasion of his 75th birthday.

‡ Electronic supplementary information (ESI) available: NMR, IR and Raman spectroscopy; further crystallographic, model calculations and analytical results; Hofmeister series. See DOI: 10.1039/b604557j

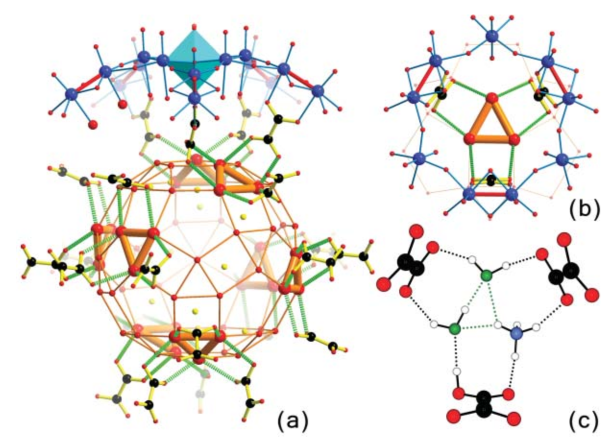

Fig. 2 (a) The interior of the capsule **3a** showing its connection to a segment of the spherical polyoxomolybdate skeleton with one of the six $\{Mo_2\}$ linkers carrying H_2O molecules (enlarged red spheres; see formula **3a**) instead of an oxalate ligands. The basic part is, geometrically speaking, the (distorted) X_{60} type Archimedean solid (brown), the corners of which are formed by H_2O and NH_4^+ on the related partially occupied 60 positions; only eight of the 20 triangles corresponding to the eight present $(H_2O)_2NH_4^+$ units lying below the pores at the C_3 axes are highlighted (in brown, bold). The hydrogen bonds between the oxalate ligand O atoms (C black, O red) and atoms of the triangles are emphasised (green lines). Additionally shown is the other type of encapsulated NH_4^+ ions (yellow spheres); (b) view of one pore situation with one $(H_2O)_2NH_4^+$ unit interacting with three "oxalates" (colours as in (a)); (c) computed H-bond pattern obtained by minimising the internal energy for the triangular unit $(H_2O)_2NH_4^+$ of **3a** in a system of three (only one protonated) oxalate groups, which leads to a minimisation of charge differences (oxalate O red, water O green, C black, N blue, H white). The optimal hydrogen bond situation has been calculated employing the PACHA formalism.[6b]‡ A comparison with cyclic $\{H_2O\}_3$ trimers would be especially interesting.[6c]

formation of **3a** – can also be proven simply by ^1H NMR: solutions of **2** and **3** of equal concentrations in DMF-d_7 were measured under the same conditions at 223 K. Compared to **2a**, the signal intensity of the oxalate proton of **3** at 13.12 ppm is significantly decreased. In the present context a study of Andrade and Taube[6d] should be referred to: the authors investigated the acid and the aquation equilibrium of $[(NH_3)_5Co^{III}C_2O_4H]^{2+}$ in aqueous medium and discussed the influence of the charge on the metal centre. The comparison shows that the monoprotonated oxalate ligand of **2a** under confined conditions is rather acidic. (Note: water molecules and small cations can pass through the capsule pores.[6e])

Remarkably, **3a** shows in its cavity, according to the present X-ray crystallography study, 60 (underoccupied) positions (Fig. 2a) which build up a distorted Archimedean solid, *i.e.* the rhombicosidodecahedron. This is formed by the encapsulated H_2O/NH_4^+ guests, comprising the characteristic faces, *i.e.* besides the 20 chemically relevant triangles (with corresponding short edges), 12 pentagons and 30 rectangles. The underoccupation is due to the fact that only eight trimers, $(H_2O)_2/(NH_4^+)$, can be present because of geometrical restrictions (see ref. 6*f*). Furthermore, in **3a** there is one set of 12 positions located below the rectangles of the mentioned distorted Archimedean solid having an occupation factor of 0.5. This type of position should be assigned to NH_4^+ ions (there might be a small contribution of H_2O molecules in agreement with the comparably large thermal ellipsoids) because (i) it has the same short distance of *ca.* 2.9 Å to the two different O atoms of the same "free" carboxylate group, which corresponds to the situation in many oxalato complexes,[7a] and (ii) it corresponds exactly to the capsule type position at which in many cases metal cations could be identified by X-ray crystallography.[1–5]

Further information on the encapsulates is derived from NMR investigations and model calculations (Fig. 2). The ^{15}N-HSQC-NMR spectrum of a solution of **3** in DMSO to which $(^{15}NH_4)Br$ was added proves the unequivocal presence of (at least) two kinds of encapsulated NH_4^+ ions in agreement with the results of our single crystal X-ray study (Fig. 3). The spectrum shows cross peaks due to the entrance of $^{15}NH_4^+$ into the capsule, *i.e.* due to an exchange with the $^{14}NH_4^+$ present in the capsule **3a** (for this type of cation transport flexibility of the sulfate ligands is necessary, which was first considered in ref. 7*b*).

The deprotonated carboxylate groups in **3a** are attractors/receptors for cations, and interact strongly *via* H-bonding with the encapsulated water molecules and especially with the ammonium ions. This leads to the presence of just eight $(H_2O)_2NH_4^+$ trinuclear units "linked" to eight oxalate ligand groups each containing three oxalates with one being protonated (Fig. 2). The addition of more than one ammonium ion per triangle is not favourable due to a $NH_4^+\cdots NH_4^+$ repulsion.

The results of the present study dealing with the electrolyte influence, *i.e.* in the form of oxalates and NH_4^+ ions on "water structures" under confined conditions might be correlated to some aspects of the Hofmeister series for anions and cations that reflect their different ordering power on the surrounding water medium.[5a]‡ The ionic sequence of the series spreads from stabilising "cosmotropes" to disrupting "chaotropes" (for related information including general problems of water structures, see ref. 8). Small and highly charged ions (cosmotropes) cause well defined structuring, *i.e.* symmetrical oriented water molecules in their neighbourhood (therefore the name!).‡ In the present situation, we have the interesting case of a cationic (NH_4^+) and clear anionic function (deprotonated oxalic acid), which hinders the formation

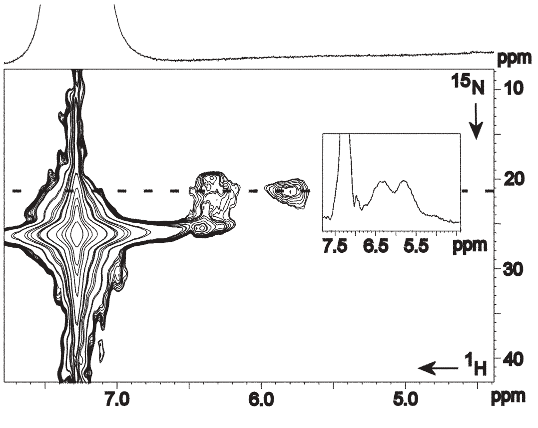

Fig. 3 ^{15}N-HSQC spectrum (^{15}N-decoupled) of **3** in DMSO. The spectrum exhibits additional peaks besides the correlation signal for the free ammonium ions (7.3/26 ppm) with exclusively upfield ^1H (6.3 and 5.8 ppm) and ^{15}N chemical shifts (21.5 ppm). The insert is the 1D spectrum of the trace at ~21.5 ppm (dotted line) to demonstrate that there is a minimum between the two additional signals.

of well defined large pure water structures/shells like in $\{H_2O\}_{100}$ and $\{H_2O\}_{80}$ found in the case where sulfate ligands (coordinated in a bidentate fashion to the $\{Mo_2\}^{2+}$ linkers) have no anionic function as they have two terminal doubly bonded O atoms with low(!) electron density and therefore negligible directing power.[5b,c]

The use of dicarboxylate ligands with "free" non-coordinating deprotonated acidic groups in our capsules opens perspectives for studying structuring processes in which encapsulated water/electrolyte hybrids are generated. The generation of the deprotonated forms is especially important because of their high directing power. Based on the present results, it becomes also feasible to study the selectivity of encapsulated ions for specific recognitions based on oxalates on a molecular scale, for instance with Ca^{2+} ions, where the interactions are known to be quite strong.[9]

We thank Prof. D. Rehder (Hamburg) for helpful discussions. L. T. thanks the Graduiertenkolleg "Strukturbildungsprozesse" of the University of Bielefeld for a fellowship.

Notes and references

§ *Synthesis of* **2**: A solution of **1**[4] (2.0 g, 0.07 mmol) and $C_2H_2O_4 \cdot 2H_2O$ (1.0 g, 7.9 mmol) in 50 ml water is stirred for 2 hours (pH < 2). After addition of NH_4Cl (2.0 g, 37 mmol) and further stirring for 10 minutes the solution is filtered and kept in a 250 ml beaker under open conditions for crystallisation at room temperature. The brown rhombohedral crystals which precipitate after three days are filtered off through a glass frit (D2), washed with ice-cold ethanol and diethyl ether, and finally dried in air. Yield: 1.2 g (59% based on Mo). Note: the crystals used for the X-ray diffraction were not washed. Anal. calcd for **2** (%): C 2.74, H 3.04, N 2.10; found: C 2.8, H 2.8, N 2.4% (see ESI‡).

Synthesis of **3**: A solution of **2** (1.0 g, 0.035 mmol) and NH_4Cl (1.5 g, 28 mmol) in 50 ml water is stirred for 1 hour (pH ≈ 2) and is then kept in an open 250 ml beaker for crystallisation at room temperature. The brown rhombohedral crystals which precipitate after 3 days are filtered off through a glass frit (D2), washed with ice-cold ethanol and diethyl ether, and finally dried in air. Yield: 0.8 g (79% based on Mo). Note: the crystals used for the X-ray diffraction were not washed.

Because of the high solubility of **2** and **3** one gets the crystals only if a rather large amount of water has been evaporated. There is an error limit regarding the number of deprotonated/protonated oxalate ligands of **3**; the number given is calculated according to the nitrogen/(NH_4^+) value obtained from the elemental analysis while the total number of oxalates is obtained from X-ray crystallography and the C-value. Whereas in **3a** the total number of encapsulated NH_4^+ could be given (within a small error limit), this is not the case for the encapsulated H_2O molecules as some are found disordered in the central part of the cavity (*i.e.* below the mentioned shells).

Anal. calcd for **3** (%): C 2.08, H 3.22, N 2.63; found: C 2.1, H 2.9, N 2.5% (see ESI‡).

¶ Structurally well defined water/electrolyte structures as found in **3** are not present in **2** because of the non-symmetrical positions of the H atoms of the ligands as well as the (probable) presence of a very few oxalic acid molecules in its cavity (see formula; anionic forms should not occur in the negatively charged capsule). Important: there is indication for disordered molecules from the X-ray study. The partial deprotonation in **3** refers to the speciation for the equilibrium between the mono- and non-deprotonated form in water (equilibrium constant $K \approx 10^{-1}$: ref. 13). During the dissolution of **2** the oxalic acid molecules are, besides some of the "oxalate" ligands, released while the latter event opens the pores drastically.

‖ *Crystal data for* **2**: $C_{64}H_{946}Mo_{132}N_{42}O_{872}$, M = 28926.7 g mol^{-1}, rhombohedral, space group $R\bar{3}$, a = 32.6802 (8), c = 73.440 (2) Å, V = 67926 (3) Å^3. Z = 3, ρ = 2.121 g cm^{-3}, μ = 1.884 mm^{-1}, F(000) = 42432, crystal size = 0.20 × 0.20 × 0.12 mm, T = 188(2) K. Total reflections 136068 ($1.66 < \theta < 26.99°$), 32868 unique (R(int) = 0.0310). The structure was refined using SHELXL-97 to R = 0.0453 for 26266 reflections with $I > 2\sigma(I)$, R = 0.0614 for all reflections. CCDC 297963. *Crystal data for* **3**: $C_{48}H_{984}Mo_{132}N_{52}O_{852}$, M = 28592.9 g mol^{-1}, rhombohedral, space group $R\bar{3}$, a = 32.6616 (8), c = 73.307 (3) Å, V = 67725 (3) Å^3, Z = 3, ρ = 2.103 g cm^{-3}, μ = 1.886 mm^{-1}, F(000) = 41988, crystal size = 0.50 × 0.40 × 0.40 mm, T = 183(2) K. Total reflections 111107 ($1.47 < \theta < 27.00°$), 31558 unique (R(int) = 0.0354). The structure was refined using SHELXL-97 to R = 0.0475 for 25654 reflections with $I > 2\sigma(I)$, R = 0.0641 for all reflections. CCDC 277334. For crystallographic data in CIF or other electronic format see DOI: 10.1039/b604557j

1 L. Cronin, in *Comprehensive Coordination Chemistry II*, ed. J. A. McCleverty and T. J. Meyer, Elsevier, Amsterdam, 2004, vol. 7, p. 1.

2 (*a*) A. Müller, P. Kögerler and C. Kuhlmann, *Chem. Commun.*, 1999, 1347; (*b*) A. Müller and S. Roy, *Coord. Chem. Rev.*, 2003, **245**, 153.

3 M. Gross, *Chem. Br.*, 2003, **39**, 8, 18; M. Gross, *Chemistry World*, 2004, **1**, Nov. Issue, 18.

4 (*a*) L. Cronin, E. Diemann and A. Müller, in *Inorganic Experiments*, ed. J. D. Woollins, Wiley-VCH, Weinheim, 2003, p. 340; (*b*) A. Müller, S. K. Das, E. Krickemeyer and C. Kuhlmann, *Inorg. Synth.*, 2004, **34**, 191.

5 (*a*) A. Müller, E. Krickemeyer, H. Bögge, M. Schmidtmann, B. Botar and M. O. Talismanova, *Angew. Chem., Int. Ed.*, 2003, **42**, 2085; (*b*) M. Henry, H. Bögge, E. Diemann and A. Müller, *J. Mol. Liq.*, 2005, **118**, 155; (*c*) A. Müller, E. Krickemeyer, H. Bögge, M. Schmidtmann, S. Roy and A. Berkle, *Angew. Chem., Int. Ed.*, 2002, **41**, 3604.

6 (*a*) I. D. Brown, in *Structure and Bonding in Crystals*, ed. M. O'Keeffe and A. Navrotsky, Academic Press, New York, 1981, vol. II, p. 1; (*b*) This gives excellent results in verifiable cases: M. Henry, *ChemPhysChem*, 2002, **3**, 561; M. Henry, *ChemPhysChem*, 2002, **3**, 607; (*c*) O. Mó, M. Yáñez and J. Elguero, *J. Chem. Phys.*, 1992, **97**, 6628; S. S. Xantheas and T. H. Dunning, Jr., *J. Chem. Phys.*, 1993, **99**, 8774; (*d*) C. Andrade and H. Taube, *Inorg. Chem.*, 1966, **5**, 1087; (*e*) E. T. K. Haupt, C. Wontorra, D. Rehder and A. Müller, *Chem. Commun.*, 2005, 391; (*f*) A. Müller, S. K. Das, S. Talismanov, S. Roy, E. Beckmann, H. Bögge, M. Schmidtmann, A. Merca, A. Berkle, L. Allouche, Y. Zhou and L. Zhang, *Angew. Chem., Int. Ed.*, 2003, **42**, 5039.

7 (*a*) C. Oldham, in *Comprehensive Coordination Chemistry*, ed. G. Wilkinson, R. D. Gillard and J. A. McCleverty, Pergamon, Oxford, 1987, vol. 2, ch. 15.6, p. 435; (*b*) D. Rehder, E. T. K. Haupt, H. Bögge and A. Müller, *Chem. Asian. J.*, 2006, DOI: 10.1002/asia.200600035.

8 F. Franks, *Water: a matrix of life*, The Royal Society of Chemistry, Cambridge, 2nd edn. 2000, p. 77; P. Ball, *H_2O: A Biography of Water*, Weidenfeld & Nicolson, London, 1999, p. 238; P. E. Mason, G. W. Neilson, J. E. Enderby, M.-L. Saboungi, C. E. Dempsey, A. D. MacKerell, Jr. and J. W. Brady, *J. Am. Chem. Soc.*, 2004, **126**, 11462; V. A. Parsegian, *Nature*, 1995, **378**, 335; R. L. Baldwin, *Biophys. J.*, 1996, **71**, 2056; P. E. Mason, G. W. Neilson, C. E. Dempsey, A. C. Barnes and J. M. Cruickshank, *Proc. Natl. Acad. Sci. USA*, 2003, **100**, 4557.

9 This is in context with the low solubility of $Ca(oxalate)_2$, which should be responsible for limited Ca^{2+} uptake in the intestine. On the other hand, oxalate occurs, besides Ca^{2+}, in animal fluids and is primarily derived from the metabolism of sugar and amino acids as an end-product. Higher concentrations of oxalates are toxic, causing hyperoxaluria.[10] Though in animal fluids metal cation (like Ca^{2+} and Mg^{2+}) interactions with proteins appear to dominate, metal oxalate binding also occurs.[11,12] Furthermore, metal cation complexation by oxalic acid occurs in different microorganisms; see ref. 12.

10 C. J. Danpure and P. E. Purdue, Primary Hyperoxaluria, in *The Metabolic and Molecular Bases of Inherited Disease*, ed. C. R. Scriver, A. L. Beaudet, W. S. Sly and D. Valle, McGraw-Hill, New York, 7th edn., 1995.

11 See the crystal structure of the bis(Mg^{2+})-ATP-oxalate complex of the rabbit muscle pyruvate kinase: T. M. Larsen, M. M. Benning, I. Rayment and G. H. Reed, *Biochemistry*, 1998, **37**, 6247. But in that case where the oxalate binds to glu271, asp295 and Mg^{2+}, the electrolytes were only added to the crystallisation medium.

12 S. H. Laurie, in *Comprehensive Coordination Chemistry*, ed. G. Wilkinson, R. D. Gillard and J. A. McCleverty, Pergamon, Oxford, 1987, vol. 2, ch. 22, p. 959.

13 F. A. Carey, *Organic Chemistry*, McGraw-Hill, New York, 5th edn, 2003, ch. 19, p. 736.

^{15}N NMR spectrum

The measurement was performed with 0.7 ml of a saturated solution of **3** in DMSO, to which 70 mg of nearly isotopically pure ($^{15}NH_4$)Br (98%) was added. The solvent was chosen because the interpretation of the spectra in water would otherwise have been more difficult due to an increased H^+ exchange. The gradient selected ^{15}N-HSQC spectrum was measured with the sensitivity enhanced version of the pulse sequence on a Bruker AVANCE 400 spectrometer, adjusted to a ^{1}H-^{15}N coupling constant of 75 Hz. The measurement time was 14 h with 64 scans and 256 increments (see also: L. E. Kay, P. Keifer and T. Saarinen, *J. Amer. Chem. Soc.*, 1992, **114**, 10663-10665).

IR and Raman spectra

Compound **2**

IR bands: ν/cm^{-1} (KBr pellet, some characteristic bands for 1700-500 cm^{-1}), ≈ 1737sh, ≈ 1707sh, ≈ 1681sh [ν_a(C=O)]; 1633s [$\delta(H_2O)$]; 1400s [$\delta(NH_4)$]; 1327w, 1248w [ν_s(C-O)]; 974s, 943w [ν(Mo=O)]; 858m, 800s, 729s, 634w, 572s.

Characteristic Raman bands: ν/cm^{-1} (solid state, KBr dilution, λ_e = 1064 nm): 944m [ν(Mo=O)]; 879s [ν_s (O_{bri} - breathing/A_{1g})]; 374m; 309w.

Compound **3**

IR bands: ν/cm^{-1} (KBr pellet, some characteristic bands for 1700-500 cm^{-1}); ≈ 1735sh, ≈ 1705sh, ≈ 1682sh [ν_a(C=O)]; 1622m [$\delta(H_2O)$]; 1400s [$\delta(NH_4)$]; 1327w, 1269w [ν_s(C-O)]; 974s, 941w [ν(Mo=O)]; 856m, 802s, 729s, 634w, 572s.

Characteristic Raman bands: ν/cm^{-1} (solid state, KBr dilution, λ_e = 1064 nm): 944m [ν(Mo=O)]; 879s [ν_s (O_{bri} - breathing/A_{1g})]; 375m; 310w.

X-ray crystallography

Crystal data for **2**: $C_{64}H_{946}Mo_{132}N_{42}O_{872}$, M = 28926.7 g mol^{-1}, rhombohedral, space group $R\bar{3}$, a = 32.6802 (8), c = 73.440 (2) Å, V = 67926 (3) Å^3, Z = 3, ρ = 2.121 g/cm^3, μ = 1.884 mm^{-1}, F (000) = 42432, crystal size = 0.20 x 0.20 x 0.12 mm^3. Crystals of **2** were removed from the mother liquor and immediately cooled to 188(2) K on a Bruker AXS SMART diffractometer (three circle goniometer with 1K CCD detector, Mo-K$_\alpha$ radiation, graphite monochromator; hemisphere data collection in ω at 0.3° scan width in three runs with 606, 435 and 230 frames (ϕ = 0, 88 and 180°) at a detector distance of 5.00 cm). A total of 136068 reflections (1.66 < θ < 26.99°) were collected of which 32868 reflections were unique (*R*(int)= 0.0310). An empirical absorption correction using equivalent reflections was performed with the program SADABS 2.10. The structure was solved with the program SHELXS-97 and refined using SHELXL-97 to *R* = 0.0453 for 26266 reflections with $I > 2\sigma(I)$, *R* = 0.0614 for all reflections; max./min. residual electron density 1.98 and –1.19 e Å^{-3}.

Crystal data for **3**: $C_{48}H_{984}Mo_{132}N_{52}O_{852}$, *M* = 28592.9 g mol^{-1}, rhombohedral, space group R$\bar{3}$, *a* = 32.6616 (8), *c* = 73.307 (3) Å, *V* = 67725 (3) Å^3, *Z* = 3, ρ = 2.103 g/cm^3, μ = 1.886 mm^{-1}, *F* (000) = 41988, crystal size = 0.50 x 0.40 x 0.40 mm^3. Crystals of **3** were removed from the mother liquor and immediately cooled to 183(2) K on a Bruker AXS SMART diffractometer (three circle goniometer with 1K CCD detector, Mo-K$_\alpha$ radiation, graphite monochromator; hemisphere data collection in ω at 0.3° scan width in three runs with 606, 435 and 230 frames (ϕ = 0, 88 and 180°) at a detector distance of 5.00 cm). A total of 111107 reflections (1.47 < θ < 27.00°) were collected of which 31558 reflections were unique (*R*(int)= 0.0354). An empirical absorption correction using equivalent reflections was performed with the program SADABS 2.10. The structure was solved with the program SHELXS-97 and refined using SHELXL-97 to *R* = 0.0475 for 25654 reflections with $I > 2\sigma(I)$, *R* = 0.0641 for all reflections; max./min. residual electron density 1.23 and –0.96 e Å^{-3}.

(SHELXS/L, SADABS from G. M. Sheldrick, University of Göttingen, 1997/2003; structure graphics with DIAMOND 2.1/3.0, http://www.crystalimpact.com/ and with POV-Ray™ 3.6 , http://www.povray.org/).
CCDC 297963 and 277334 contain the supplementary crystallographic data for **2** and **3** respectively. These data can be obtained free of charge from The Cambridge Crystallographic Data Centre *via* http://www.ccdc.cam.ac.uk/data_request/cif .

Analytical details

The chemical formulae of **2** and **3** refer to the maximum possible number of water molecules and are calculated from the respective cell volumes and the sum of volumes of all cell ingredients excluding those of the crystal water molecules. The given calculated values for C, N, H are related to a formula with 50 crystal water molecules less than given (note: **2** and **3** as all similar compounds show slow weathering, *i.e.* loss of crystal water). The (small number of) disordered/encapsulated oxalic acid molecules in **2a** cannot be determined.

Additional information about the Hofmeister Series

1) The series describes, according to the original discovery, the order of effectiveness of different ions in stabilising a protein and their ability to salt the protein out.

2) Strongly hydrated ions considerably increase the difference between the hydrogen bond donating and accepting capacity of the linked water molecules resulting in the breakdown of the water network. Now it is evident that the understanding of the effects of cationic and anionic solutes on protein behaviour in solution which was originally considered by Hofmeister only phenomenologically, requires a deeper understanding of the interaction of water molecules with the specific solutes' architectures; see ref. 8 and M. Chaplin, Water Structure: http://www.lsbu.ac.uk/water/

3) The cation ''behaviour'' in the present type of nanocontainers[5a] can be correlated with the (not fully understood) Hofmeister series while anions hydrate more strongly than cations as in case of the same ionic radius the hydrogen atoms can approach closer in anions (see: T. E. Creighton, *Proteins: Structures and Molecular Properties*, Freeman, New York, 2nd edn, 1997, pp. 156, 263–264, 295–296; A. A. Zavitsas, *J. Chem. Phys. B*, 2001, **105**, 7805).

Model calculations

A central $(H_2O)_2NH_4^+$ triangular H-bond pattern with an average H-bond energy of -16 kJ mol^{-1} is found embedded in a larger and much stiffer six-membered ring with an average H-bond energy of -81 kJ mol^{-1}.

Chapter 3

Summary and conclusion

Coordination chemistry especially of the transition metals is an important area of chemical research as it shows tremendous interdisciplinary relevance, e.g. for catalysis and for bioinorganic chemistry including even aspects of medicine regarding therapy as well as diagnosis [1]. In this context, coordination chemistry studies under confined conditions seem to be of special importance. One unique class of the coordination chemistry is presented by the polyoxometalates which can be considered as soluble metal-oxide fragments with an enormous structural variety and a multitude of interesting properties. The present thesis is dealing with self-assembly processes of polyoxomolybdates but also with performing well-defined reactions at well-defined sites of the structurally well-defined but very complex metal oxide-based nanoobjects.

The new type of inclusion species $\{Mo_{146}\}$ comprising 16 encapsulated K^+ and SO_4^{2-} ions shows an unusual 64-membered $\{K(SO_4)\}_{16}$ ring integrated into a wheel-shaped type nanocluster host:

$$K_{14}Na_{16}[Mo_{114}^{VI}Mo_{32}^{V}O_{429}(H_2O)_{50}\{KSO_4\}_{16}] \cdot ca.500H_2O \quad \mathbf{1}$$

The nanosized system in question is formed by synergetically induced functional complementarity and represents a text-book example of a very complex non-biological material. Moreover, the present cluster system offers the potential to act polytopically for different substrates thus allowing, in principle, the study of ring-structures-based complex cooperative effects between different guests like cations and anions.

It is possible to construct spherical-shaped polyoxomolybdate structures designed so that they behave as artificial cells as they allow to model passive biological ion transport as well as cell response to stimuli. Based on the compound:

$$(H^+OC(NH_2)_2)_{23}(NH_4)_{29-n}[\{(H^+OC(NH_2)_2)_{20} + (H_2O)_{81-n} + (NH_4)_n\} \subset \\ \{(Mo^{VI})Mo_5^{VI}O_{21}(H_2O)_6\}_{12}\{Mo_2^VO_4(SO_4)\}_{30}] \cdot ca.100H_2O \quad \mathbf{2}$$

---

[1] J.A. McCleverty, T.B. Meyer (Eds.), *Comprehensive Coordination Chemistry II*, Elsevier, Oxford, **2003**; W. Kaim, B. Schwederski, *Bioinorganic Chemistry: Inorganic Elements in the Chemistry of Life: An Introduction and Guide*, Wiley, Chichester, **1994**; S.J. Lippard, J.M. Berg, *Principles of Bioinorganic Chemistry*, University Science Books, Mill Valley, CA, USA, **1994**; J.M. Thomas, W.J. Thomas, *Principles and Practice of Heterogeneous Catalysis*,Wiley-VCH,Weinheim, Germany, **1997**.

where the protonated urea corks are gating the porous capsule, an interesting phenomenon could be studied. In nature, the cell cannels are not continuously open and ions can pass through only when the channel is open; the same is happening with our polyoxomolybdate spherical system when it is exposed in aqueous solution to Ca^{2+} ions; the temporary release of the corks allow the uptake of the calcium cations which finally lead to the precipitation of the mentioned compound:

$$(H^+OC(NH_2)_2)_{15}(NH_4)_{23-n}[\{(H^+OC(NH_2)_2)_{20} + Ca_8 + (H_2O)_{60} + (NH_4)_n\} \subset \\ \{(Mo^{VI})Mo_5^{VI}O_{21}(H_2O)_6\}_{12}\{Mo_2^VO_4(SO_4)\}_{30}] \cdot ca.150H_2O \;\; \mathbf{3}$$

It was possible to fine-tune the functionalities of the interior surface of soluble, porous spherical capsules based on the rather robust fundamental skeleton $\{Pentagon\}_{12}\{Linker\}_{30} = [\{(Mo^{VI})Mo_5^{VI}O_{21}(H_2O)_6\}_{12}\{Mo_2^VO_4(ligand)\}_{30}]^{n-}$ (e.g. for ligand = acetate, n = 42- [2]). The modifications of the cluster interiors are carried out by exchanging the ligands coordinated to the 30 $\{Mo_2\}$ linkers, in the present case by substituting the acetate ligands with dicarboxylates.

$$(NH_4)_{42}[\{(Mo^{VI})Mo_5^{VI}O_{21}(H_2O)_6\}_{12}\{Mo_2^VO_4(OOCCOOH)\}_{30}] \\ \cdot ca.\{300H_2O + 2C_2H_2O_4\} \;\; \mathbf{4}$$

$$(NH_4)_{38}[\{(H_2O)_x + (NH_4)_{14}\} \subset \{(Mo^{VI})Mo_5^{VI}O_{21}(H_2O)_6\}_{12} \\ \{Mo_2^VO_4(OOCCOOH)\}_8\{Mo_2^VO_4(OOCCOO)\}_{16}\{Mo_2^VO_4(H_2O)_2\}_6] \\ \cdot ca.\ (300-x)\ H_2O \;\; \mathbf{5}$$

Whereas **4** shows at the 30 equivalent linker positions 30 identical monoprotonated oxalate ligands, **5** shows unprecedented internal structural features as a result of the internal surface. The deprotonated carboxylate groups in **5** are attractors/receptors for cations, and interact strongly *via* H-bonding with the encapsulated water molecules and especially with the ammonium ions. This leads to the presence of just eight $(H_2O)_2(NH_4)$ trinuclear units "linked" to eight oxalate ligand groups each containing three oxalates with one being protonated. These types of assemblies are of general interest for understanding hydration abilities in chemical and especially biochemical systems. The results of the present study dealing with electrolyte influence on "water structures" under confined conditions might be correlated to some aspects of the Hofmeister series for anions and cations that reflect their different ordering power on the surrounding water medium. The use of bifunctional ligands with "free" non-coordinating especially deprotonated groups in our capsules opens perspectives for studying structuring processes in which encapsulated water/electrolyte hybrids are involved while this procedure may be extended to magnetic metal ion aggregates, too.

---

[2] (a) L. Cronin, E. Diemann, A. Müller in *Inorganic Experiments* (Ed.: J. D. Woollins), Wiley-VCH, Weinheim, **2003**, p. 340; (b) A. Müller; S. K. Das, E. Krickemeyer, C. Kuhlmann, *Inorg. Synth.*, **2004**, 34 (Ed.: J. Shapley), p. 191.

Chapter 4

Curriculum Vitae

CURRICULUM VITAE

LIVIU-DAN TOMA

ADDRESS

Karlstraße 37
64283, Darmstadt
Germany
Phone: +49-(0)-6151-5990087
Mobil: +49-(0)-179-9707936
Email: liviu_toma@yahoo.com

PERSONAL DETAILS

Date of birth: 2nd of December, 1976
Place of birth: Tirgoviste, Romania
Nationality: Romanian
Marital status: Married

WORKING EXPERIENCE

01/2006–	Research Associate, Technische Universität Darmstadt, Fachbereich Material- und Geowissenschaften, Fachgebiet Disperse Feststoffe, Petersenstr. 23, D-64287 Darmstadt, http://www.tu-darmstadt.de/fb/ms/fg/df/index.html Main activities and responsibilities: Involved in the project "Ceramic Temperature and Pressure Sensors based on Molecularly Derived SiOC Ceramics by Injection Moulding Process" part of the Priority Programme 1181 "Nanoscaled Inorganic Materials by Molecular Design: New Materials for Advanced Technologies".
01/2002–10/2005	Research Assistant, Department of Inorganic Chemistry, Fakultät für Chemie der Universität Bielefeld, Postfach 10 01 31 - D-33501 Bielefeld, http://www.uni-bielefeld.de/chemie/ac1/ Main activities and responsibilities: Developed new methods for the synthesis of nanometer-scale inorganic molecules and clusters which belong to the family

	of polyoxomolybdates.
02/2001–09/2001	Research Assistant, Departament de Química Inorgànica/Instituto de Ciencia Molecular, Facultat de Química de la Universitat de València, Dr. Moliner 50, 46100 Burjassot (València), Spain, http://www.uv.es/%7Eicmol/index.html Main activities and responsibilities: Synthesis, crystal structures and magnetic properties of cyanide- and phenolate-bridged tetranuclear complexes.
01/2000–08/2000	Assistant Professor, Chemistry, Lumina Educational Institution High School, B-dul Energeticienilor nr. 9-11, sec. 3, Bucharest, Romania, http://www.isb.ro Main activities and responsibilities: Involved in teaching at High School level.
10/1998–12/2000	Student, Inorganic Chemistry Laboratory, Faculty of Chemistry, University of Bucharest, Str. Dumbrava Rosie nr. 23, 020464, Bucharest, Romania, http://www.unibuc.ro/en/home Main activities and responsibilities: undergraduate research in the projects: ”Supramolecular architectures in the material science”, CNCSU, Type C, No. 30; and ”New strategies of synthesis of molecular magnetic materials”, MCT, Gr 4116/B9; supervised by Prof. Dr. Marius Andruh. Synthesis of bi- and multinuclear complexes used for the design of heteropolymetalics systems used as precursors for the synthesis of molecular magnetic materials.

EDUCATION

2005	Expected to finish Dr.rer.nat.; Field: Chemistry and Nanoscience; Institute: University of Bielefeld, Bielefeld, Germany. Duration: January 2002 – November 2005. Thesis Title: Polyoxomolybdates with Emergent Properties.
2001	Completed MSc; Field: Coordination Chemistry; Institute: University of Bucharest, Bucharest, Romania. Duration: October 1999 – June 2001. Thesis Title: Robson Ligands: building-blocks from a dynamic library used for the design of heteropolymetalics systems.
1999	Completed BSc; Field: Chemistry, Specialization in Inorganic Chemistry; Department of French Language, Graduation from the Psychology-Pedagogy module. Institute: University of Bucharest, Bucharest, Romania. Duration: October 1995 – June 1999.
1995	Completed Baccalaureate; Vladimir Streinu High School, Gaesti, Romania. Duration: September 1991 – June 1995.

FELLOWSHIPS AND AWARDS

2002	Fellowship from DFG Graduiertenkolleg 223 ”Strukturbildungsprozesse”, Bielefeld, Germany. Duration: March 2002 – February 2005.

2001	Erasmus Fellowship, University of Valencia, Spain. Duration: February 2001 – September 2001.
1999-2000	National Merit Scholarship for graduate education, Romania.
1998	First prize, Scientific session of communications, November, University of Bucharest, Romania.
1995-1999	National Merit Scholarship for undergraduate education, Romania.

List of publications

[1] L. M. Toma, R. Lescouëzec, **L. Toma**, F. Lloret, M. Julve, J. Vaissermann and M. Andruh, *J. Chem. Soc., Dalton Trans.*, **2002**, 3171.

[2] A. Müller, **L. Toma**, H. Bögge, M. Schmidtmann and P. Kögerler, *Chem. Commun.* **2003**, 2000.

[3] **L. Toma**, L. M. Toma, R. Lescouëzec, D. Armentano, G. D. Munno, M. Andruh, J. Cano, F. Lloret and M. Julve, *J. Chem. Soc., Dalton Trans.*, **2005**, 1357.

[4] L. M. Toma, **L. D. Toma**, F. S. Delgado, C. Ruiz-Pérezb, J. Sletten, J. Cano, J. M. Clemente-Juan, F. Lloret and M. Julve, *Coord. Chem. Rev.* **2006**, 250, 2176.

[5] A. Müller, **L. Toma**, H. Bögge, C. Schäffer and A. Stammler, *Angew. Chem. Int. Ed.*, **2005**, 44, 7757.

[6] A. Müller, **L. Toma**, H. Bögge, M. Henry, E. T. K. Haupt, A. Mix and F. L. Sousa, *Chem. Commun.*, **2006**, 3396.

Conferences and lectures, poster presentation

- ”Modeling Receptors for Specific Substrates, Encapsulation and Networking in Porous Materials”, **Liviu Toma**, short lecture at the 5.rd *Workshop Graduate School of Chemistry and Biochemistry*, 19./20.01.2004, Zentrum für Interdisziplinäre Forschung (ZIF), Bielefeld, Germany.
- ”Well Defined Reactions at Well Defined Position of Nano Objects”, **Liviu Toma**, short lecture at the 3.rd *Workshop Graduate School of Chemistry and Biochemistry*, 20./21.01.2003, Zentrum für Interdisziplinäre Forschung (ZIF), Bielefeld, Germany.
- ”A Novel Supramolecular Species with an Encapsulated 64-Membered Ring Comprising Potassium and Sulfate Ions: Rational Manipulation of Ring-Shaped Nanoobjects with Option for Integration of Paramagnetic Centers”, **L. Toma**, A. Müller, H. Bögge, M. Schmidtmann, P. Kögerler, poster, *Eight International Conferences on Molecule-based Magnets*, ICMM’2002, Valencia (Spain) 5-10 October.
- ”Moleculars systems heteropolimetallics obtained by the coupling of binuclears complexes of Cu(II) and Ni(II) with hexacianometalats”, G. Grasa, R. Gheorghe, D. Visinescu, **L. Toma**, M. Andruh, poster, *25th National Session of Chemistry*, Calimanesti Caciulata, Valcea, 1999, Romania.